Environmental Science
Water Research & Technology

CRITICAL REVIEW

Cite this: *Environ. Sci.: Water Res. Technol.*, 2021, **7**, 1895

Macroscopic covalent organic framework architectures for water remediation

Abdul Khayum Mohammed [a] and Dinesh Shetty *[ab]

Covalent organic frameworks (COFs) are two- (2D) or three-dimensional (3D) crystalline and porous polymers constructed from organic molecules with various symmetries. The reticular synthetic strategy and the dynamic covalent chemistry of COFs allow the construction of regular intrinsic pores with stable functional covalent pore walls. The unique chemical structural features of COFs promote excellent molecular adsorption from various environments, especially from water. In this regard, COFs have been explored for their water remediation ability to a wide range of pollutants including persistent organic pollutants, toxic metals, radio-active wastes, *etc.* Notably, the development of COFs into various macrophysical forms such as foams and thick and thin-film membranes led to a new direction of advanced level water treatment. In this review, we have discussed the progress of the macroscopic architecture of COFs for water purification research. The notable shift from the granular adsorption of molecular pollutants to rapid and efficient foam-based adsorption and size and chemo-selective membrane-based separation is highlighted in this review. Finally, we have discussed our perspective on the future of this area of research for the next level of remediation technology of polluted water.

Received 15th June 2021,
Accepted 13th September 2021

DOI: 10.1039/d1ew00408e

rsc.li/es-water

Water impact

In the present era of scarcity of water resources, effective treatment of wastewater is a significant prerequisite for a growing economy. However, the progress of the aqueous remediation sector highly depends on the structural development of the material. Therefore, this review is focused on the macroscopic developments of covalent organic frameworks for the removal of emerging toxic contaminants from water.

1. Introduction

As the primary source of life, water plays a critical role in sustainability and continuous progress of society. The availability of pure water is limited (3%) compared to its overall distribution on earth surfaces (70%) because of impractical utility sources like glaciers and seawater. The available water sources have severe contamination issues due to the heavy deposition of industrial waste, urbanization, and mismanagements. By 2050, it is estimated that 3 to 4 billion people in the world would confront the worse situation of a lack of pure water for drinking and other household utilities.[1] The contamination is due to the presence of organic or inorganic molecules, radioactive substances, microorganisms, or any other toxic agents (Fig. 1b).[2] These pollutants can be soluble, partially soluble or insoluble which depends on their chemical structures. Many organic and inorganic micropollutants are highly soluble in water due to the efficient hydration of the molecules.[3,4] Regardless of the solubility properties of pollutants, the potential contaminations with their inherent toxicity are capable of destroying the valuable benefits of water. In this regard, it is highly required to remediate the polluted water into purified water.

Porous materials are found to be the adsorptive platform for micropollutant molecules considering their physical and chemical interactions on a large surface area (Fig. 1a).[5] Porous carbon is one of the cheapest and primitive adsorptive cleaning agents of polluted water and has been used for a long time.[6,7] Porous carbon has been further developed into advanced nanostructured materials, such as two-dimensional (2D) graphene and one-dimensional (1D) carbon nanotubes, and widely investigated as an efficient water purification adsorbent and membrane material.[8] Zeolites are another class of porous materials made from three-dimensional (3D) aluminosilicates for softening polluted water.[9,10] However, the limitations in the structural

[a] *Department of Chemistry, Khalifa University of Science and Technology, 127788 Abu Dhabi, United Arab Emirates. E-mail: dinesh.shetty@ku.ac.in*
[b] *Center for Catalysis and Separations (CeCaS), Khalifa University of Science and Technology, 127788 Abu Dhabi, United Arab Emirates*

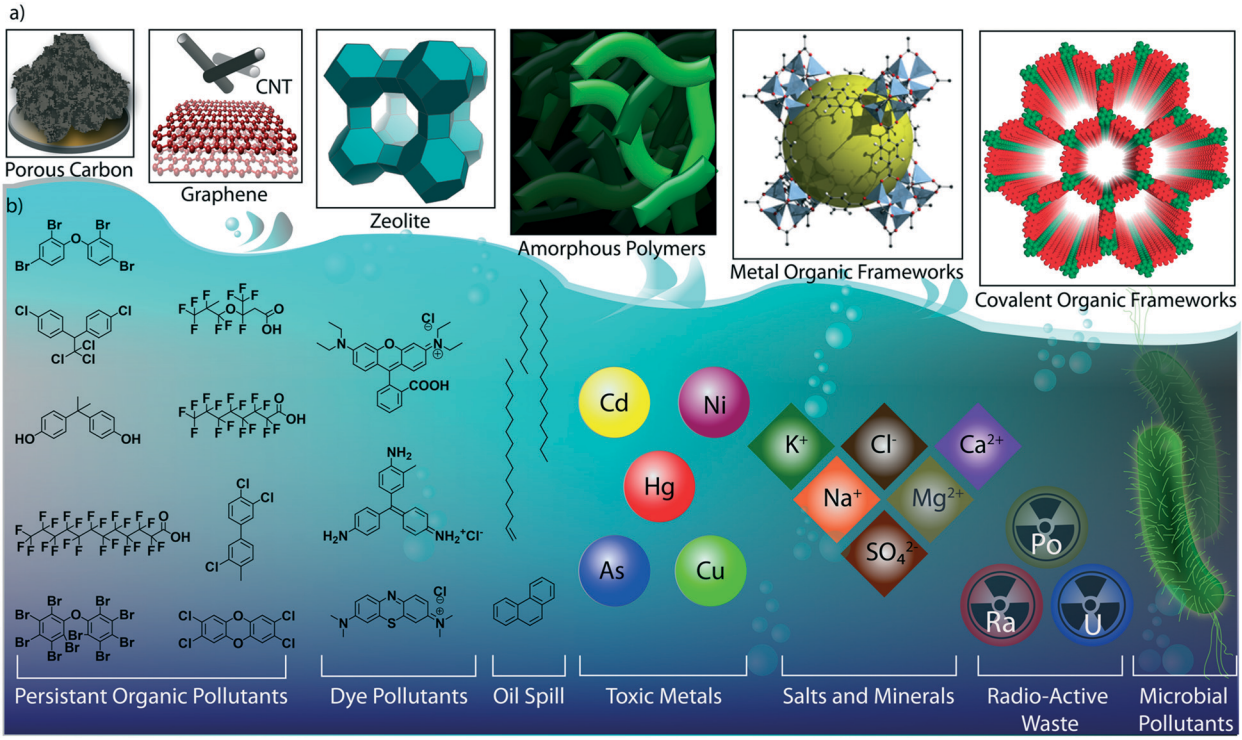

Fig. 1 Porous materials and various micropollutants. a) The various porous materials used for water remediation application. b) The library of micropollutants in water.

diversity of such porous materials narrow the efficient and selective removal of micropollutants from water. Although recently developed amorphous porous polymers possess functional diversity,[11–13] the lack of ordered porosity is one of the main challenges in overcoming the separation difficulties of chemically diverse pollutant molecules. Moreover, the emergence of reticular porous materials such as metal–organic frameworks (MOFs)[14,15] and covalent organic frameworks (COFs) has opened a wide window of opportunities for water purification.[16–18] MOFs have been

Abdul Khayum Mohammed

Dr. Abdul Khayum Mohammed received his B.Sc. and M.Sc. degrees in chemistry from St. Thomas College, Trichur (2012) and Cochin University of Science and Technology (CUSAT), Cochin (2014), India, respectively. After qualifying for all India joint CSIR-UGC National Eligibility Test (NET-JRF), he moved to CSIR-National Chemical Laboratory, Pune, to pursue his Ph.D. (with Dr. Ulhas Kharul and Dr. Rahul Banerjee) and received his degree in 2019. Currently, he is working as a postdoctoral researcher in Dr. Dinesh Shetty's group at the chemistry department of Khalifa University, Abu Dhabi. His current research focuses on developing macroarchitectures of crystalline organic polymers for energy and separation applications.

Dinesh Shetty

Dr. Dinesh Shetty holds a Ph.D. degree (2011) in chemistry from Seoul National University, Korea. He pursued postdoctoral research at Emory University, USA, and Institute for Basic Science, POSTECH, Korea, before moving to New York University Abu Dhabi to work as a research scientist. In 2019, he started an independent career at Khalifa University, Abu Dhabi. He is a trained chemist with hands-on experience in multidisciplinary research areas, including materials science, porous materials, and supramolecular chemistry. He is the recipient of the Young Investigator Award from both the Korean Society of Nuclear Medicine and the Korean Cancer Research Foundation. In his free time, he writes poems and newspaper column articles, and podcasts his thoughts. His research interest is focused on developing multifunctional polymers for various applications, including energy and water purification.

widely investigated for their excellent capturing efficiency towards diverse types of toxic molecules and ions in water.[19–21] While MOFs are composed of metal knots and organic linkers, COFs are organic structures with lightweight elements. In COFs, the pre-designed organic building blocks are connected through strong covalent bonds and are arranged in the designated 2D or 3D order (Fig. 2). Reticular organic chemistry offers to create permanent ordered porosity with desired shape and size. Moreover, the pore walls can be decorated with desired functional blocks.

The unique structural features of COFs offer opportunities for efficient low-energy filtration of molecular pollutants from water. The strategic selection of COFs for target-specific micropollutants strongly depends on the correlated physical and chemical properties between the COF and pollutant molecules. In general, the reticular design of 1D, 2D, and 3D structures of COFs with desired functionality and continuously ordered porosity is the most important feature for water purification application. We will discuss the properties of COFs in the next section of this review for a detailed overview of the advantages of COFs.

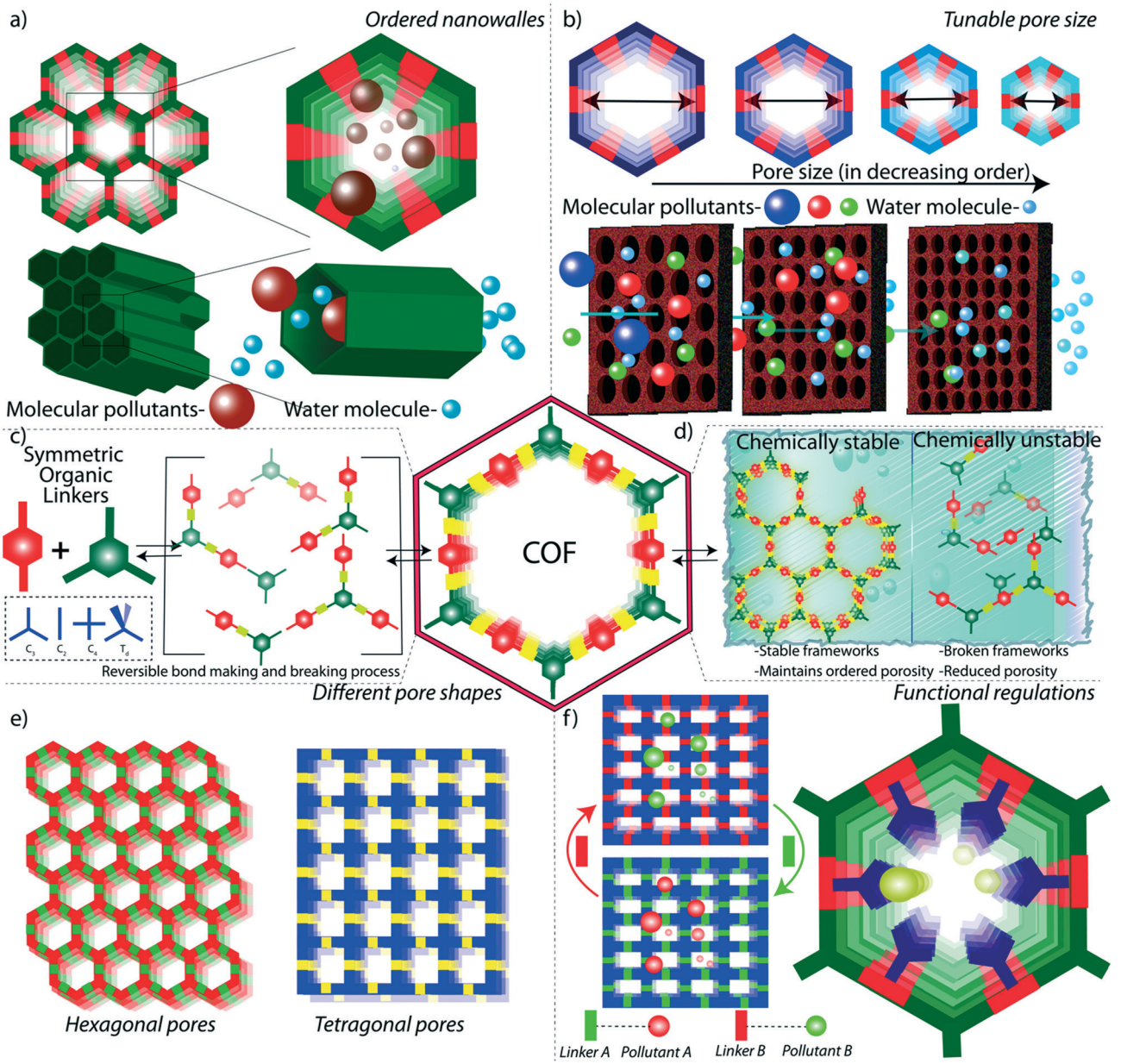

Fig. 2 The chemical and physical features of a COF. a) The ordered porous structure of the COF promotes the lucid diffusion of molecules. b) The size-selective molecular diffusion through tuning of pore size in the COF. c) The dynamic covalent chemistry of symmetric organic linkers leads to the formation of crystalline COFs. d) The chemical stability of the COF in an aqueous environment. The chemically stable COF maintains the ordered porosity, whereas unstable COFs are broken into framework fragments and ordered porosity no longer exists. e) The reticular chemistry allows the fabrication of different shapes of pores in the COF. f) The chemical functional control over the frameworks determines the molecular uptake into the COF.

It is important to note that the number of reports on COF or COF hybrid-based water purification is increasing each year exponentially. Recently, many research outputs have been published owing to the potential features of COFs. The available reviews on COF-based water remediation mostly dealt with the fundamental design principles of the chemical structures of COFs.[22,23] However, there is no review available in the literature for understanding the macro structural progress of COFs for water treatment application. Meanwhile, the progress of the aqueous remediation sector highly depends on the structural development of the material. Taking all these aspects, in this review, we specifically focused on the macroscopic developments of COFs for the removal of emerging toxic contaminants from water. In the first section, we discuss the effect of chemical and physical features of COFs in water purification which provides an overview of nano and macro structure–property relationships. In the later section, we have highlighted the journey of COFs from their granular nature into 2D membranes and hierarchical 3D porous foams. The macrophysical structural evolution has been demonstrated with the progress in the purification performance of a large library of micropollutants from water.

2. Chemical properties of COFs for pollutant removal

In general, the symmetric organization of molecules through intermolecular bonding results in ordered crystalline materials. The formation of regular patterning of molecules through weak non-covalent interactions and coordinate bonding is highly feasible due to the ease of self-error correction in the crystallization process. Meanwhile, the higher bond strength (~340 kJ per mole) of covalent bonds restricts the ordered formation of such extended molecular periodic structures. A novel concept was introduced by Yaghi and co-workers in 2005 by applying reversible dynamic covalent bonds between symmetric molecules that led to the extended regular growth of covalently bonded organic frameworks.[24]

The final topology of the COF is directly connected to the symmetry of the building blocks and reaction conditions.[25–27] The symmetry (*ex*: linear, diagonal, trigonal, tetrahedral, hexagonal, and other complex symmetries) is a major factor in deciding the shape and size of the porous structure of the material. The topology can decide the physical features of COFs, which will be detailed in the next section.

Although the porous features of COFs mainly originate from the topology of the material, the chemical properties of COFs depend on their molecular building blocks and the nature of connecting bonds. The strategic connection of two or more building units in a 1D/2D/3D framework provides a precise integration and maximum exposure of molecules in a solid heterogeneous surface. The periodic appearance of the molecules in the porous matrix is a result of dynamic covalent bond formation between the building units under thermodynamically and kinetically controlled reactions (Fig. 2c).[28] In general, the connectivity of the building blocks in COFs is critically important to the stability and functional diversity of the material.

The fabrication of COFs was first achieved through the connection of C_2 symmetric boronic acid aromatic linkers into six-membered boroxine units. In subsequent years, various boronic ester-linked COFs have been synthesized.[24] Despite the poor chemical stability, these COFs are well known for their good crystallinity and porosity. Later, imine (–C═N–), azine (–C═N–N–C–) and hydrazone (–C═N–NH–) chemistry was successfully implemented for the synthesis of 2D and 3D-COFs. The imine linkages are chemically stable in water compared to the boronic ester bonds.[26,29–31] However, most of these networks are labile in strong acid and basic medium that results in the disintegration of the frameworks. In this regard, the conversion of –C═N– into –C–N– in the framework is desired to design chemically robust frameworks. Such *in situ* conversions by β-keto–enol tautomerism offer a large library of chemically stable COFs.[32]

Covalent triazine frameworks (CTFs) are a class of 2D-COFs with an abundant presence of nitrogen atoms.[33] The Lewis acid ($ZnCl_2$) catalyzed cyclotrimerization reactions of nitrile (C≡N) functional groups at high temperatures (~400 °C) often yield good porous but semi-crystalline materials. The rich nitrogen contents in the conjugated framework have been successfully utilized for heterogeneous catalysis and energy storage applications. However, the limited availability of functionally diverse organic building blocks is one of the main concerns in the progress of CTFs.

In contrast to the heteroatom linked bonds in COFs, the sp^2 carbon connected frameworks are of much interest owing to their robust chemical stability and improved electronic conductivity. The first cyano substituted vinylene connected 2D-COF was fabricated in 2016 through the Knoevenagel condensation of 1,4-phenylenediacetonitrile and 1,3,5-tris(4-formylphenyl)benzene as symmetric building blocks.[34] A notable attempt to synthesize a semi-conductive olefin-linked 2D-COF was realized by the Knoevenagel condensation of 1,3,6,8-tetrakis(4-formylphenyl)pyrene and 1,4-phenylenediacetonitrile (PDAN) under solvothermal conditions.[35] The continuous effort to formulate a cyano free, unsubstituted vinylene-linked COF has led to the successful implementation of the aldol condensation reaction in a dynamic covalent chemistry approach. The first unsubstituted olefin-linked 2D-COF was reported in 2019 by connecting 2,4,6-trimethyl-1,3,5-triazine (TMT) and 4,4′-biphenyldicarbaldehyde (BPDA).[36] The chemical inertness of the olefin linkage in a range of pH values could be an important factor for the development of next-generation water purification materials.

2.1 Chemical functional diversity

Weak chemical interactions play a critical role in the remediation of water from various micropollutants.

Adsorptive or membrane platforms provide a suitable chemical environment to capture guest molecules through weak interactions such as hydrogen bonding, pi-pi, and dispersion interactions.[37] The reticular design of COFs aids the precise integration of suitable chemical functionalities into the porous matrix. The ordered porosity in COFs enhances the accessibility of decorated functional moieties towards the pollutants (Fig. 2a). The chemical moieties are connected to the framework through the pre-designed framework and/or post-synthetic modification.[38] In the pre-designed networks, the organic building blocks with desired chemical functionalities are directly used. However, in some cases, it would be difficult to form a framework with desired functionalities through direct synthesis. In such cases, researchers adopt the post-synthetic modification of the synthesized framework, which allows dynamic opportunities to graft a large library of functional moieties on pore walls and the surface of the framework. However, the post-synthetic modifications of COFs result in partial functionalization of the network and/or decrease in porosity of the resultant material. It is well investigated that the fine control over the functional moieties largely affects the properties of the COFs in different applications including catalysis, gas storage, energy storage, and water purification.[29,39–44]

In low energy remediation, the pollutants are removed from water mainly through four different mechanisms: 1) adsorption, 2) ion exchange, 3) molecular sieving, and 4) chemical reaction-based detoxification. In adsorption, the molecules are adsorbed on a porous platform through weak interactions. In this regard, it is important to facilitate the interactions between the framework and pollutants (Fig. 2f). For example, the COFs that were designed as acidic could easily interact with basic molecular pollutants through acid–base interactions and *vice versa*. Likewise, a COF was decorated with thioether units that could selectively interact with mercury metal ions in water through Hg–S weak chemical bonding. Ion exchange is another method to purify water from ionic pollutants which requires ionic porous platforms to exchange cations and anions. Molecular sieving is a widely adopted separation strategy in membrane-based water filtration. In the chemical reaction method, the organic contaminants in water are subjected to COF-based oxidation or catalytic processes, which degrade the toxic molecules into non-toxic fragments.

The design principles of membranes should be in line with the higher flux rate and efficient rejection of pollutant molecules during the separation process. The size-selective rejection of molecules largely depends on the pore sizes in the membranes (Fig. 2b and e). Meanwhile, the flux rate of the water molecules is commercially important and can be largely controlled by the chemical construction of the membrane. The regulation of the hydrophilicity in the membrane largely improves the flux rate of water through the pores. The hydrophilicity enhances the interaction of the water molecules with the membrane at the molecular level, boosts the rapid diffusion of the water molecules through the pores and mitigates membrane fouling. It is theoretically demonstrated that the integration of $-NHCOCH_2CH_2NH_2$, $-OCH_2CH_2CH_2OH$, and $-NHCOCH_2-COOH$ into the TpPa-1 COF enhances the flux rate of water.[45] The water flux was enhanced by 92% in an amine rich COF thin film coated on a membrane compared to its pristine counterpart. The hydrophilicity can also be improved in COFs through the introduction of imine and enamine linkers in the framework.[46]

2.2 Chemical stability of the framework

Since the frameworks are constructed by a reversible chemical reaction, it is of utmost importance to have structural stability in a polluted water environment. The decomposition of the framework leads to the partial or complete destruction of the ordered structure, which adversely affects water purification (Fig. 2d).[47] In this regard, the COFs for water remediation purposes should possess chemical stability in an aqueous medium for a wide range of pH values. The boronic-ester-linked COFs are highly prone to decomposition of their frameworks even at atmospheric humidity due to the Lewis acidic nature at boron ester centers.[48] Researchers have developed an alkyl functionalization strategy to improve the chemical stability of the boronic ester COFs (COF-18 Å).[49] The pore wall functionalized alkyl groups protect the boron from the attack of water molecules by the hydrophobic effects of alkyl chains (methyl, ethyl, and propyl). Although the aqueous stability of the COFs has been enhanced, the surface area was decreased drastically which limits the pollutant adsorption ability. Moreover, even partial decomposition of COFs negatively impacts water purification by releasing the decomposed molecular fragments into the water.

In another method, pyridine vapor doping in COF-10 increased the hydrolytic stability of the framework through the direct protection of boron centers by basic pyridine molecules.[50] The pyridine-modified COF-10 maintains its crystallinity for seven days under continuous humid air treatment. However, the higher concentration of pyridine destroys the framework stability due to the acid–base chemical reaction. Due to the presence of acidic or basic pollutants, the pH of the water mostly falls in the acidic or basic range. In this regard, the chemical robustness of COFs under such harsh conditions is a critical factor for proper utilization in water purification. The decomposition of an imine-linked COF under acidic conditions has been rectified by the introduction of intramolecular hydrogen bonding into the framework. The COF has been constructed from symmetric building blocks 2,5-dihydroxyterephthalaldehyde (C_2) and 5,10,15,20-tetrakis(4-aminophenyl)-21*H*,23*H*-porphine) (C_4).[51] In this enol–imine chemical structure, the hydroxyl functional group interacted with imine nitrogen through intramolecular hydrogen bonding. This interaction helps the framework to maintain its planarity through the molecular

locking of the building units. The improved planarity of the imine-linked COF further enhances the crystallinity and porosity of the material. Moreover, the intramolecular hydrogen bonding effectively protects the imine bond from proton attack under acidic conditions. As a result, the imine linked DhaTph COF exhibits higher chemical stability (3 N HCl) compared to the non-molecular locked DmaTph COF. Although the intramolecular hydrogen-bonded imine-linked COF displays acidic chemical stability, it is important to improve the framework robustness towards basic conditions as well. The introduction of β-keto–enol tautomerism into the 2D framework of the COF largely enhanced the chemical stability of the material under both acidic and basic conditions without compromising the porosity and crystallinity.[32] During the crystallization of the COF, the framework was irreversibly converted from the enol to keto form through proton tautomerization. The enamine bonds are chemically inert towards acidic and basic conditions compared to the imine bond. The β-ketoenamine frameworks display good chemical stability in 9 N HCl and 9 N NaOH for seven days. The chemical stability of imine-linked 2D-COFs has also been drastically improved through the integration of the methoxy (–OMe) functional group into the framework.[52] In this strategy, 2,5-dimethoxyterepthaldehyde (DMTA) has been strategically chosen as a methoxy bearing C_2 symmetrical linker to construct a 1,3,5-tris(4-aminophenyl)-benzene (TAPB) based 2D-COF through Schiff base synthesis. In general, the partial polarization of the imine bond in COFs (*i.e.*, δ^+ charge in C and δ^- charge in N) results in interlayer repulsion and consequent poor π–π interaction between the COF layers. In contrast, the methoxy-bearing imine-linked COF is free from such interlayer repulsion due to the inductive effect of –OMe functional group (+I effect) and protects the framework from the acidic and basic environment. The resonance effect enhances the chemical stability of the imine-linked COF under harsh conditions (12 N HCl or 14 N NaOH or in various protic and aprotic solvents).

Recently, a benzoxazole-linked COF has been demonstrated for its excellent chemical stability due to bond inertness under harsh conditions.[53] Again, the chemical stability of imine-linked COF was improved through the introduction of a C_3 linker 2,4,6-trimethoxy-1,3,5-benzenetricarbaldehyde (TpOMe) into the 2D framework through the solid-state mixing strategy.[54] The methoxy (–OMe) group is believed to participate in the interlayer interaction with the imine nitrogen in the neighboring layer. The weak interlayer interaction has been demonstrated theoretically, *i.e.*, the C–H from the –OMe group has been hydrogen-bonded with the electronegative nitrogen in the imine bond with a distance of ~2.07–2.2 Å. The interlayer C–H···N hydrogen bonding induces steric and hydrophobic effects around the imine (C═N) bonds, which makes them chemically inert under harsh acidic and basic conditions. Notably, these TpOMe-based imine-linked COFs are chemically stable in conc. H_2SO_4 (18 M), conc. HCl (12 M), and NaOH (9 M). In another interesting report, a novel polyarylether-based 2D-COF was constructed from *ortho*-difluoro benzene and catechol building units.[55] In this design strategy, the nucleophilic aromatic substitution reaction of symmetrical linkers leads to the formation of chemically strong ether linkages. As a result, the ether-linked 2D-COFs exhibit robust chemical stability in a harsh chemical environment. The chemical inertness of the ether linkage maintains the framework stability without structural decomposition in boiling water, HCl (12 M), H_2SO_4 (18 M), NaOH (14 M), HF (40%), and chromic acid solution. Recently, metal incorporation supramolecular engineering of a hydrazone-linked 2D-COF was demonstrated with improved chemical stability in various polar organic solvents.[56] In this strategy, the supramolecular coordination of metal ions into the nitrogen moieties in the open channels of COFs hindered the bond rotation and enhanced the structural stability.

The chemical stability of COFs towards electro or photo redox reactions is important in various advanced water treatment methods. The lower oxidation–reduction stability of COFs in aqueous medium causes the degradation of the frameworks, which results in the self-pollution of water. Importantly, the chemical linkage of COFs enhances the redox stability in electro and photo reactions. For example, a chemically stable redox-active anthraquinone stitched β-ketoenamine 2D-COF has been reported for its electrochemical proton charge storage characteristics.[42] It shows continuous 2500–5000 cycles of redox stability towards a potential window of 1 V in water. The chemical stability was enhanced by the introduction of interlayer C–H···N hydrogen bonding.[57] Similarly, a hydroquinone β-ketoenamine 2D-COF exhibited redox stability in a potential range of 0.2 V to 1.8 V *vs.* Zn/Zn^{2+}. The excellent cyclic stability (>100 000 redox cycles) of the COF in 3 M H_2SO_4 in a potential window of 1 V signified the importance of the chemical stability of frameworks in redox-active reactions.[43] Furthermore, β-ketoenamine 2D-COFs were successfully applied for catalytic purposes in photo-induced reactions. For instance, a recent development on a COF–Mxene hybrid system for the photocatalytic hydrogen evolution reaction verified the significance of structural stability in photocatalytic oxidation reactions.[58]

3. Physical properties of COFs for pollutant removal

3.1 Porosity features

Physical features like porosity and macroscopic forms are critical factors of COFs for advanced level purification of water. In general, the porosity of the material plays the primary role in the adsorption and molecular sieving of micropollutants from water. The porosity is a measure of void spaces in a material, which enhances the surface area for functional activities in storage and filtration applications. However, most of the porous materials are amorphous in nature, *i.e.*, a random distribution of pores. The amorphous

nature of porous materials limits their potential properties like rapid, selective, and efficient adsorption capabilities. Notably, the dynamic covalent chemistry of COFs creates an ordered porosity with a regular pore size distribution (Fig. 2c). Herein, the porosity has been constructed by the consecutive symmetrical arrangement of organic linkers during the crystallization process of COFs.

The pollutant removal from water is benefited from the ordered porosity of COFs in three different ways: 1) it improves the efficiency of the adsorption or ion exchange of pollutants. Because of the ordered nature, the active surface area of the COFs is well exposed to the aqueous pollutant environment with minimum blocking of pores. As a result, the maximum surfaces of the COFs are accessible to the adsorption of molecular pollutants hence improving the efficiency of purification. 2) The ordered porosity enhances the rapid uptake of the molecular pollutants from water. Unlike amorphous materials, the inner core pores are not blocked in COFs which allows instant molecular diffusion through the entire porous matrix. 3) The ordered porosity with a uniform distribution of pore sizes rules the selective removal of molecular pollutants from contaminated water. Along with the chemical functionalities, the ordered porosity with tunable pore size helps the selective removal of molecules according to their sizes. In the design principles, the pore sizes have been controlled by the strategic selection of building units with varying sizes and symmetry. Apart from the control over the reticular design, the pore sizes have been controlled through the post-synthetic functionalization of the pore walls, which depends on the length and bulkiness of the attached functional moieties. It is successfully demonstrated in an azide bearing diboronic acid (N_3-BDBA) and benzene diboronic acid (BDBA) based 2D-COF.[59] The azide units were post-modified into the various functional groups through the click reaction with alkyne moieties. In this transformation, the pore sizes are reduced from 3 nm to 1.2 nm upon 5 to 100% post chemical transformation. The precise control over the pore sizes with uniform distribution greatly helps the selective molecular sieving of the pollutants. The design of the optimum pore-size COF is a critical step in the fabrication of ultra or nanofiltration membranes for the selective rejection of molecules as well as for higher solvent flux rates. For instance, COFs with 2–3 nm pore size are suitable to remove large size dye molecules (>3 nm) from water while maintaining enough flux rate.[44,60] The lower pore dimensions mitigate the flow of water through the COF membranes which adversely affects the economically viable purification. In contrast, desalination membranes required smaller pore sizes to remove salts and minerals from water.[46] In terms of pre- and post-design advantages, it is possible to fabricate COF membranes with desired pore sizes for targeted purification purposes. In addition to the induction of single uniform pores, the reticular design strategy also allows the fabrication of multiple pores or heteropores in COFs.[61] In this strategy, two or more symmetrical building units have been used for dynamic assembly bond formation for the construction of hetero-linked COFs with ordered multiple pores. In addition to the dimensional pore construction, the symmetric assembly of organic linkers offers to build the desired shape and size of the pores. Again, the pore shape depends on the symmetry of the building blocks.[62] For example, C_2 and C_4 linkers form tetragonal pores, whereas C_3 and C_2 linkers result in hexagonal-shaped pores. These porosity features made COFs ideal for the remediation of water from various pollutants such as persistent organic pollutants, dye molecules, salts, and heavy metals.

3.2 Macroscopic developments of COFs

The judicial placement of atoms or molecules into the desired macro-physical forms is of great interest for advanced level purification of water. The macroscopic architecture development of porous materials into granular form, foams, thin films, or membranes is utilized for functionally diverse water treatment applications. Importantly, the fabricated macrophysical forms of COFs exhibit their inherent properties such as the precise and ordered placements of the molecules, regular nanochannels, low-weight density, and thermal and chemical stability (Fig. 3). COFs are generally featured as granular forms in the earlier developments of the material (Fig. 3a).[18] The conventional solvothermal or microwave-assisted synthesis results in COFs of granular nature. It could be due to the nanocrystalline particles in granular COFs showing poor interaction with each other. Although granular COFs exhibit excellent porosity as well as crystallinity, they lack hierarchical porosity in the range from meso to macro dimensions due to the absence of higher-order defects and fewer self-assembled pores. On this ground, COFs were constructed as foams or aerogels with hierarchical porosity with pore dimensions ranging from micro to macro for the efficient and rapid uptake of organic and inorganic micropollutants from water (Fig. 3b).[63,64] Notably, the macrophysical forms like powder and foams of COFs are generally used for the adsorption-based purification of water. Although adsorption methods are known for their low-energy and efficient purification, the commercial interest of water treatment requires membrane-based separations due to their higher selectivity, the ease of bulk level direct separation, and regeneration of the material.[65] Researchers have attempted to fabricate COFs into two-dimensional thin films or membranes through various strategies. The support-based bottom-up synthesis was one of the earliest notable attempts to achieve the oriented growth of 2D COF thin films.[66] The boronic ester-linked COF-5 thin film was deposited on single-layer graphene on different substrates such as silica, silicon carbide, and copper using this method. The crystalline COF-5 was vertically stacked on the graphene layers with a thickness of 132 ± 18 nm. Similarly, the anthraquinone-linked β-ketoenamine DAAQ-TFP COF was fabricated on a gold thin-film with a thickness of 200–1000 nm through the slow addition of monomers.[67] The

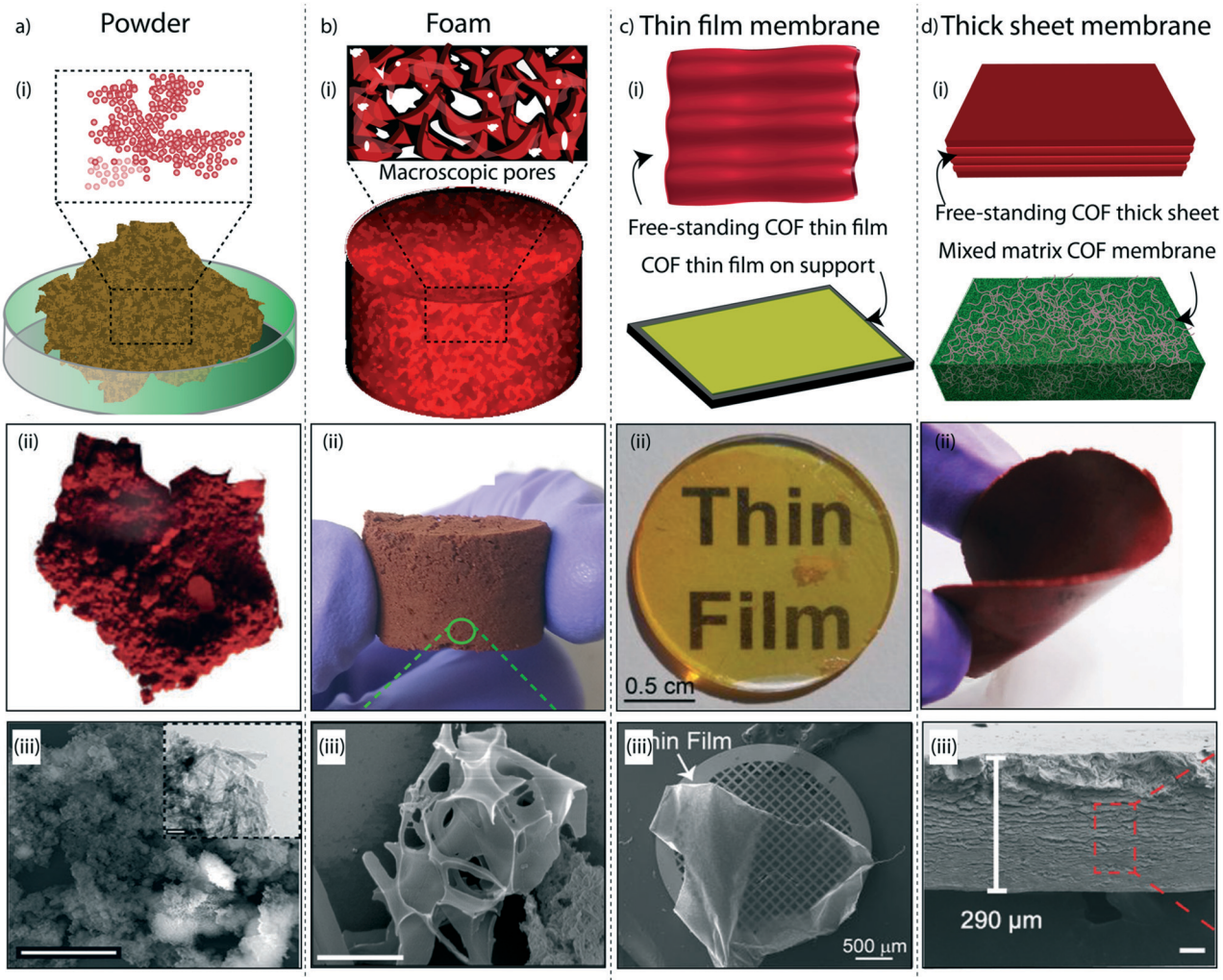

Fig. 3 The macroscopic development of COFs. a) (i) The graphical representation, (ii) digital image, and (iii) SEM and TEM images of a granular COF. b) (i) The graphical representation, (ii) digital image, and (iii) SEM image of a COF foam. c) (i) The graphical representation, (ii) digital image, and (iii) SEM image of a COF thin-film membrane on a support. d) (i) The graphical representation, (ii) digital image, and (iii) SEM image of a free-standing membrane. [Reproduced from ref. 51 (Fig. 3aii and iii) and ref. 28 (Fig. 3dii and iii) with permission from John Wiley and Sons, copyright 2016. Reproduced from ref. 45 (Fig. 3bii and iii) and ref. 54 (Fig. 3cii and iii) with permission from American Chemical Society, Copyright 2019 and Copyright 2017].

macroscopic upconversion of the powder DAAQ-TFP COF into thin film improved the charge storage properties to a large extent up to 400%. In another work, a thiophene stitched COF thin film was fabricated on ITO and NiO/ITO with a thickness of 150 nm.[68] However, the lack of porosity of such systems disables the separation features for water treatment. Moreover, a chemically exfoliated β-ketoenamine COF was fabricated into a free-standing thin film at the air–water interfaces.[69] Later, the effort on the fabrication of an imine-linked COF (COF LZU) on a porous alumina tube was then introduced for the successful separation of organic micropollutants from water.[70]

Meanwhile, the macroscopic design of the COF into a free-standing membrane was a great challenge due to the crystalline nature of the material. The earlier COF membrane fabrication strategies adopted well-known mixed matrix membrane synthesis to induce the porosity and free-standing features concurrently.[71] In the fabrication of mixed matrix membranes, amorphous porous polymers are blended with crystalline and porous COFs for mechanical and porous support. Although the mixed matrix membranes work for various separation applications, the complete utilization of the potential features of COFs is limited in such systems due to heavy reduction of porosity and crystallinity during the fabrication process. In this regard, researchers have developed free-standing COF membranes composed of 100% COF crystallites for the separation of micropollutants (Fig. 3c and d). The *p*-toluenesulphonic acid (PTSA) assisted solid-state synthesis of β-ketoenamine frameworks offers the fabrication of free-standing COF membranes with a thickness of 200–300 μm for various potential separation features in wastewater treatment and regeneration of active pharmaceutical ingredients [APIs] from organic solvents.[44] The continuous effort to design nanometer thickness

membranes was successfully demonstrated by introducing interfacial polymerization of COF thin films.[72,73] In this crystalline polymerization strategy, both β-ketoenamine and imine-linked COFs were developed by independent attempts and explored for their improved micropollutant separation abilities. The story of COFs on water treatment based on their various stages of macrophysical developments will be discussed in detail in the following sections of the review.

3.3 Mechanical properties of COFs

The macroscopic shape transformation of COFs should be associated with good mechanical properties to hold the crystallites together while using them in a water medium. Unlike amorphous linear polymers, the nanocrystalline nature of COFs retards the mechanical intactness of the bulk form of the material due to the restricted flexibility of the particle assembly at the nano-level. The mutual exclusiveness of crystallinity and flexibility must be addressed for further progress of higher dimensions of COFs. Furthermore, it is crucial to fabricate 2D or 3D macroscopic forms of COFs with strong tensile strength for real-life applications, especially in water treatment. Although the mixed matrix membranes are mechanically reasonable for such utilities, the proper exploration of COF properties demands the fabrication of additive-free membranes or sheets. The enhancement of the chemical interaction between the nanocrystalline domains could be an effective strategy to improve the mechanical features of COF structures. Controlling the molecular building units in 2D-COFs could lead to the regulation of the electronic environment of the crystallites. Notably, a π electron-rich anthracene-connected 2D-COF exhibits an improved mechanical response towards various physical treatments, including bending, twisting, and stretching, compared to its counterpart (anthraquinone-linked 2D-COF).[74] Herein, the π electron-rich anthracene moieties in the COF could efficiently engage in crystallite–crystallite interaction, improving the nanodomains' mechanical strength. The stress–strain analysis of the anthracene-linked COF thin sheet displayed a 9% breaking strain, whereas the anthraquinone COF has a poor breaking strain of 2%. The modification of small molecules has further enhanced the mechanical response of COFs to polymer building units to construct the framework.[75] The interfacial polymerization of a polyethylene glycol connected COF (poly COF-42) offers improved mechanical strength of the 2D sheets. The mechanical stretching analysis showed a breaking strain of 9.5% at a higher loading of poly-linkers into the COF. Moreover, the poly-COF membranes are mechanically responsive to organic vapour. Exposure to organic vapours such as ethanol, dichloromethane, *etc.* causes bending of the membrane and retaining the original state after being in contact with organic vapour-free air. Like 2D membrane or sheets, the conservation of 3D-shapes of COFs also faces the challenge of balancing the crystallinity and the mechanical flexibility. Adding one more dimension into 3D structures brought an intriguing task to maintain the inherent properties and the mechanically resistant nature. The compressive breaking strain of 3D-printed TpBD COF foam was calculated to be 22.2%.[64] A notable enhancement in compressive breaking strain (50%) was found in COF/rGO aerogel.

The research investigation in the mechanical aspects of macroscopic COFs is still limited and needs thorough exploration of the molecular-level understanding. The bulk form of the COFs possesses varying structural defects that may cause significant fluctuations in Young's modulus values. Recent theoretical findings showed the mechanical anisotropy of 2D-COFs at the molecular level.[77] Even 3% of structural defects may be attributed to the 50% decrement in the Youngs modulus value. It suggests the road ahead to understand the mechanical behaviour of COFs from the molecular to the macroscopic level.

3.4 Electronic properties

The mechanism or mode of water remediation also depends on the electronic features of the extended covalent network of COFs. The presence of π electrons and several other fully or partially charged sites in COFs determines the interaction site of foreign molecules in an aqueous medium. The electronic properties of COFs originate from the linker and lattice symmetry and molecular building blocks and the linkage between them. The size and shape of the linker and the lattice symmetry directly control the spacing of molecules in the framework matrix of the COF. Consequently, the electron density distribution over the COF was regulated by the proper spacing of functional molecules. The structure-symmetry-electronic features were theoretically demonstrated in three-fold and four-fold nodes of COFs.[78] The three-fold symmetry offers a highly symmetric hexagonal system with nearly flat bands around the Fermi level. Meanwhile, strong band dispersion was noted for tetra-fold symmetric connected (square lattice) zinc porphyrin or pyrene and diacetylene moieties. Notably, the charge characteristics of COFs are largely influenced by the electronic features of organic building blocks. Generally, the linkers and knots of COFs are π electron-rich aromatic molecules that provide both electronic conjugation and ordered π–π stacking of 2D layers, which results in the overall charge transfer properties. Moreover, organic building blocks with anionic, cationic, and redox-active centres significantly affect the separation/adsorption of various potent toxic molecules/ions. Again, the linkage between the molecular building blocks extends or breaks the conjugation of COFs. For example, the single bond B–O in boronic ester COFs breaks the conjugation and may result in hetero-junctions. Meanwhile imine-linkages (–C═N–) outstretch the π conjugation throughout the framework. However, the polarized imine bonds retard the electronic movement through covalent bonds. Enhanced electron/hole movement was observed in olefin (C═C) connected building blocks in COFs.[35] Advanced water

remediation demands highly optimized electronic platforms for the electro or photoactive removal of pollutant molecules. The reticular approach of COFs towards the desired electronic properties could be an effective strategy for removing toxic or precious molecules or ions from aqueous media.

4. Granular COFs for water treatment

Earlier reports about 2D and 3D COFs obtained through solvothermal, ionothermal, and microwave-assisted syntheses indicate that they are generally in granular form. They have been explored as molecular adsorbents *via* the physical and/or chemical adsorption of smaller molecules from air, water, and organic solvents. The granular nature of the COFs allowed them for good dispersion in solvents and subsequent capture of molecules The molecular sieving mechanism mainly depends on the pore size and the nature of functional moieties in COFs (Fig. 4). Both factors influence adsorption, ion exchange, and chemical reaction-based pollutant degradation. The large pore size can accommodate large pollutant moieties, whereas the small pore size can selectively reject them. The functional sites induce various non-covalent and ionic interactions. The weak non-covalent interactions involve π–π bonds, hydrogen bonds, dispersion interactions, and electrostatic interactions. For example, an amine pore wall decorated β-ketoenamine framework has been constructed for the adsorption of lactic acid from water.[79] In this work, the $TpBD(NO_2)_2$ COF was chemically reduced into $TpBD(NH_2)_2$, and the amines were further modified into amides using acetic anhydride while maintaining the structural stability of the porous material. The lactic acid adsorption isotherm of $TpBD(NH_2)_2$ and $TpBD(NHCOCH_3)_2$ showed type I plots with adsorption up to 6.6 and 4.0 wt%, respectively, which was higher than the adsorption efficiency of $TpBD(NO_2)_2$ (adsorption as high as 2.5 wt%). The higher adsorption of the amine decorated COF was explained by the ability of intermolecular hydrogen bonding between $-NH_2$ and lactic acid. Detailed examples of various pollutant uptakes are discussed in the following section.

4.1 Removal of persistent organic pollutants

The adsorption–desorption properties of COFs made them an excellent platform for the recyclable removal of hazardous pollutants, especially persistent organic pollutants (POPs), from water. POPs are organic molecules that are known as 'forever chemicals' due to their persistent nature.[80] Considering their unbreakable structures, bio-magnification, and toxic features, POPs are micropollutants of major concern in the environment, especially in water. Polyfluorinated alkyl substances (PFAS) are a class of POPs, widely applied for the preparation of fluoropolymers, aqueous film-forming foams, food packages, household utilities, and various water repellents. The severe deposition of PFAS in ground and surface water causes ecological persistence and bioaccumulation that leads to dangerous health issues for living systems.[81] The pore wall functionalization of imine-linked COFs has been demonstrated to remove thirteen different PFAS molecules from water effectively.[82] The pore walls of the hexagonal imine-linked 2D-COF was functionalized with amine groups to interact with the anionic PFAS molecules (Fig. 5b). The condensation reaction between 1,3,5-tris(4-aminophenyl)-benzene and a mixture of terephthalaldehyde and dialdehyde bearing azide-functionalized ethylene glycol side chains

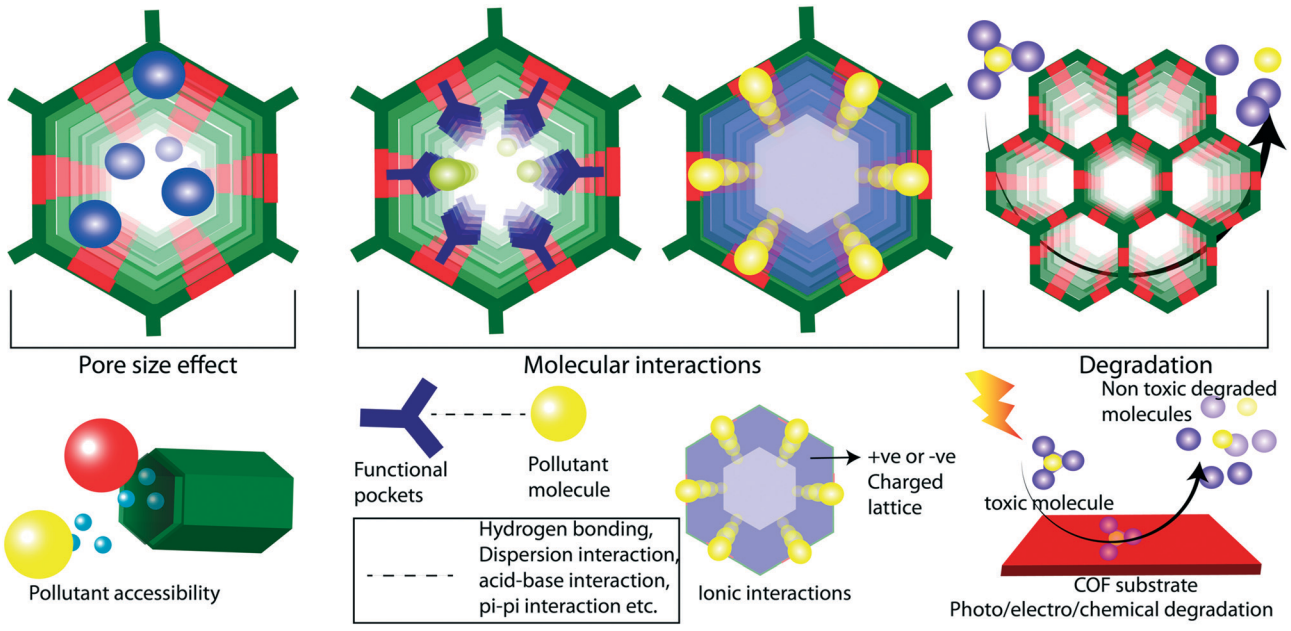

Fig. 4 Mechanism of pollutant removal/capture by COFs.

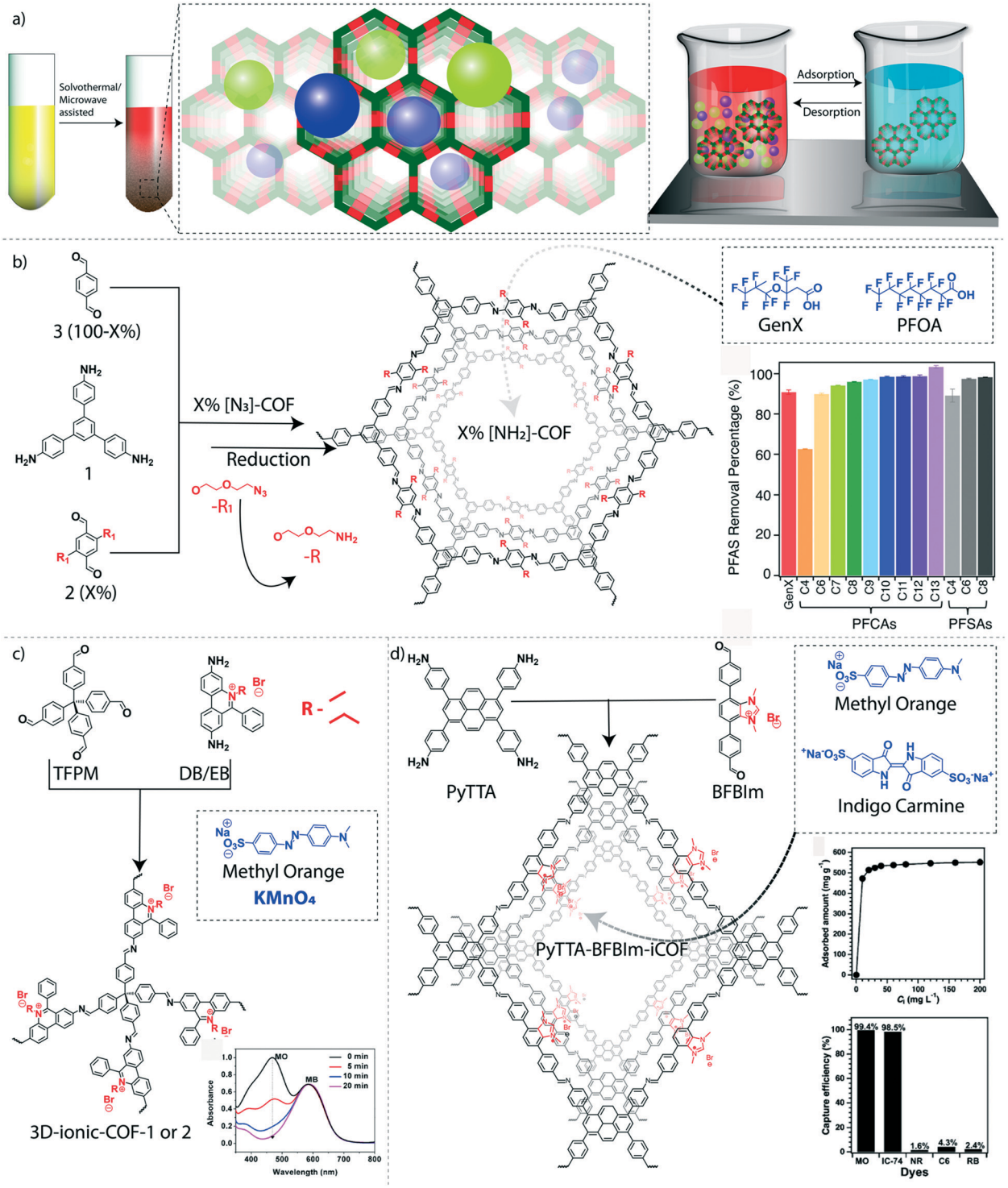

Fig. 5 Granular COFs for organic micropollutant removal from water. a) The graphical representation of the solvothermally synthesized COFs for adsorption-based water purification. b) The schematic diagram of the amine-functionalized COF for removal of GenX and perfluorinated alkyl pollutants. c) The schematic diagram of the ionic 3D-COF and the UV-spectrum of dye capturing efficiency. d) The schematic diagram of the synthesis of charged interface PyTTA–BFBIm-iCOF and dye capturing efficiency. [Reproduced from ref. 59 (Fig. 5b data) and ref. 65 (Fig. 5c data) with permission from American Chemical Society, Copyright 2018 and Copyright 2017. Reproduced from ref. 64 (Fig. 5d data) with permission from John Wiley and Sons, copyright 2017].

resulted in X%[N_3]-COFs where X ranges from 0 to 100%. Again, the azide groups were further chemically reduced to NH_2 by using PPh_3 in methanol (X%[NH_2]-COFs). The 100%[NH_2]-COF exhibits a BET surface area of 1000 m^2 g^{-1} with an average mesopore size distribution of 2.6 nm. The removal efficiencies of GenX molecules (ammonium salt of

hexafluoropropylene oxide dimer acid fluoride) were increased from 1%[NH_2]-COF (removal efficiency: 73%) to 20%[NH_2]-COF (removal efficiency: 97%). However, the removal efficiency was reduced to 56% in the case of 100%[NH_2]-COF plausibly because of the reduction of pore volume in the presence of a large number of amine groups inside the pores. The long hydrophobic alkyl chains covered most of the pore space at higher loading of the $-NH_2$ functional group, which also resulted in decreased BET surface areas. Moreover, the poor removal efficiency of 0–100%[N_3]-COFs indicates the significance of $-NH_2$ groups for the interactions with pollutant molecules. The highest adsorption of GenX molecules was found to be 240 mg g^{-1} for 20%[NH_2]-COF. The 28%[NH_2]-COF was found to be an effective adsorbent for a mixture of thirteen various PFAS with different chain lengths and functional groups in relevant concentrations in water. The COF showed remarkable removal efficiency for twelve PFAS (>90%), whereas only 63% of perfluorobutanoic acid was removed. The GenX binding isotherm fits the Langmuir model, which provides an affinity coefficient of 6.3×10^4 M^{-1} with 200 mg g^{-1} as the calculated maximum capacity for 28%[NH_2]-COF.

In 2017, an alternative adsorption-based separation methodology was developed for the removal of POPs from water that involves magnetic solid-phase extraction (MSPE) for the rapid adsorption of organic pollutants.[83] A 3D bouquet-like magnetic COF was fabricated by the integration of β-ketoenamine TpPa-1 into Fe_3O_4 nanoparticles. The synthetic strategy followed the treatment of amino-functionalized Fe_3O_4 nanoparticles with 1,3,5-triformylphloroglucinol (Tp) and subsequent reaction with both Tp and Pa-1 monomers. The covalently bonded assembly of core–shell magnetic flowers (Fe_3O_4) and porous stems (TpPa-1 COF) offered a bouquet-like morphology that enhanced the magnetic decantation of the adsorbents from water. Polycyclic aromatic hydrocarbons (PAHs) are another category of toxic and carcinogenic POPs present in the environment.[84] The major source of PAHs is the partial combustion of organic substances like petroleum. To address this problem, the Fe_3O_4–TpPa-1 magnetic COF was applied for the effective removal of six different PAHs from water. The π-frameworks and hetero-atoms (nitrogen and oxygen) present in the TpPa-1 COF are believed to be the binding sites for aromatic organic pollutants. It was found that all PAHs were recovered with a removal efficiency of 90%. Furthermore, the magnetic nanoporous materials were found to be independent of the pH of the solution and the efficiency was not affected by the varying saline concentration of the pollutant solution. Notably, the PAHs were removed with a low relative standard deviation (2–8%) from different sources including tap water, lake water, and river water. In another study, a dioxin-linked 2D-COF was constructed for the solid-phase micro extraction (SPME) of PFOA and PFOS (perfluorooctanesulphonic acid) from water.[85] The framework was built from 2,3,5,6-tetrafluoro-4-pyridinecarbonitrile with 2,3,6,7,10,11-hexahydroxy triphenylene through an irreversible nucleophilic substitution reaction. The maximum experimental adsorption capacities for PFOA and PFOS were found to be 261 mg g^{-1} and 209.5 mg g^{-1}, respectively. The adsorption rate constants (k_2) for PFOA and PFOS were 6.26 and 9.45 g mg^{-1} min^{-1} respectively.

4.2 Removal of toxic organic dyes

The commercial importance of dyes in fabrics, food, cosmetics, pharmaceuticals, and paper industries results in nearly 8 million tons of worldwide annual production. The heavy discharge of organic dyes from industries causes severe environmental pollution.[86] Considering the excellent solubility of most organic dyes in water, the extraction of these toxic organic molecules needs customized purification methods. Because of their robust chemical interactions, COFs were successfully customized as solid-phase extractors for a range of toxic dyes dissolved in water. The removal of anionic dyes was demonstrated by introducing a positive surface in 2D-COFs, which facilitates electrostatic interactions between the COF surface and dye molecules.[87] PyTTA–BFBIm-iCOF, an ionic COF, was constructed from 4,4′,4″,4‴-(pyrene-1,3,6,8-tetrayl)tetraaniline (PyTTA) and 5,6-bis(4-formylbenzyl)-1,3-dimethyl-benzimidazolium bromide (Fig. 5d). The ionic interface was created by unconventional reversed AA-stacking mode with an alternate orientation of the cationic centers to both sides of the walls. These cationic centers in the π–π stacked framework avoid the charge repulsion that allows keeping good crystallinity and permanent porosity with a BET surface area of 1532 m^2 g^{-1}. Moreover, enough space was created within the ordered pores (~2.3 nm) of the COF because of the alternative orientation of the cationic linkers. Both the spatial arrangement and the cationic surface of the material enhance the selectivity and efficiency of the removal of anionic dyes such as methyl orange (MO) and indigo carmine (IC). The rapid adsorption of MO (99.9%) with a maximum adsorption capacity of 553 mg g^{-1} was observed, which is equivalent to 0.81 MO per benzimidazolium cationic linker. However, the adsorption efficiency was slightly decreased at basic pH (95% at pH = 10 and 91% at pH = 13) because of the presence of competitive hydroxyl anions. On the other hand, the adsorption efficiency of the COF for IC was about 98.5%. The kinetic adsorption analysis of MO suggested pseudo-second-order kinetics with a high kinetic constant of 5.32×10^{-2} g mg^{-1} min^{-1}. The adsorbents were regenerated for six cycles by treatment with 1 M NaBr solution without compromising the efficiency. Moreover, the poor removal efficiency of neutral and cationic organic dyes by COF indicates its better selectivity of COF towards anionic dyes.

Notably, the cationic centers were integrated into a 3D framework that resulted in rapid, reversible, and selective anionic pollutant uptake. The cationic 3D-COFs were fabricated by using the Schiff base condensation reaction between linear cationic linkers (diimidium bromide or ethidium bromide) and a tetrahedral neutral knot (tetrakis(4-formylphenyl)methane) with a diamond topology (3D-ionic COF-1 and 3D-ionic COF-2) (Fig. 5c).[88] The tetrahedral

centers are connected with long-sized C_2-linkers resulting in the formation of interpenetrated networks. Both COFs exhibit good porosity (BET surface area: 966 m^2 g^{-1} for 3D-ionic-COF-1 and 880 m^2 g^{-1} for 3D-ionic-COF-2) and microporous nature (NLDFT pore size distribution of 8.6 Å for 3D-ionic-COF-1 and 8.2 Å for 3D-ionic-COF-2). Owing to their cationic 3D pores, these COFs were used for the size-selective removal of anionic dyes from a mixture of dyes (MO and methylene blue MB). The smaller size MO was completely removed from the mixture, whereas MB remained in the solution. Very recently, calix[4]arene-based interpenetrated and non-interpenetrated COFs with excellent cationic dye adsorption efficiency were reported.[89] Due to the highly acidic nature of integrated hydroxyl groups in calix[4]arene units, the COF has selectively removed cationic dyes (MB and rhodamine B RhB) from water. The Langmuir adsorption isotherm of the interpenetrated COF offers maximum adsorption capacities of 35 mg g^{-1} (MB) and 25 mg g^{-1} (RhB).

In general, the hetero-atom enrichment (sulfur and nitrogen) of COFs greatly improved the capture of organic dyes from water. A novel π conjugated 2D-COF (BTT–TAPT-COF) was synthesized from sulphur-rich benzo[1,2-*b*,3,4-*b*′,5,6-*b*″]trithiophene-2,5,8-tricarbaldehyde (BTT) and nitrogen-rich 1,3,5-tris-(4-aminophenyl)triazine (TAPT).[67] The hetero-atom-rich COF with a BET surface area of 864 m^2 g^{-1} exhibits excellent adsorption features toward IC at lower pH.[90] The protonation of the precisely arranged hetero-atoms enhances the electrostatic interactions with the anionic pollutants. The maximum adsorption capacity from the Langmuir model was found to be 578 mg g^{-1}. However, only moderate recyclability was achieved due to the strong interaction between the COF and dye molecules. A triazine-based fluorine COF (FLU-COF) was designed for the effective removal of sky-blue A from water.[91] The COF was synthesized from 4,4′,4″-((1,3,5-triazine-2,4,6-triyl)tris(oxy))tribenzaldehyde (TOB) and 2,7-diaminofluorene (DAF) through the hydrothermal method. The maximum adsorption capacity and the highest removal efficiency were found to be 299 mg g^{-1} and 99%, respectively. The dye molecules are adsorbed onto the FLU-COF through intermolecular hydrogen bonding with nitrogen groups and π–π interactions with 2D-layers.

In addition to chemical functional features, the porosity characteristics also influence the adsorption capacities of dye molecules. In this regard, the COFs must be designed with enough porous cavities to accommodate the dye molecules. Considering these aspects, a triazine-based 2D-COF (Ttba-TPDA) composed of 4,4′,4″-(1,3,5-triazine-2,4,6-triyl) tris(1,1′-biphenyl)trianiline (Ttba) and [1,1′:4′,1″-terphenyl]-4,4″-dicarbaldehyde (TPDA) was reported with a large pore size of 5.8 nm (surface area of 726 m^2 g^{-1}).[92] The mesoporous nature of the COF allows the effective molecular diffusion of RhB molecules into the porous matrix. The batch adsorption experiments showed a high adsorption capacity of 833 mg g^{-1}. Besides, the COF showed fast removal kinetics with an adsorption rate constant of 0.136 g mg^{-1} min^{-1}. The facile regeneration of the adsorbent over five cycles indicates its weak interaction with the dye molecules. The COF maintains the efficiency of dye adsorption in a range of pH (2 to 11) and even in the presence of salts such as NaCl and $CaCl_2$. The significance of the porosity of COFs for the uptake of dye molecules was further demonstrated by two different meso- and microporous 2D-COFs for the removal of different size organic dyes in water. The mesoporous triazine polyimide TS-COF-1 (BET surface area 1484 m^2 g^{-1}) was synthesized with a pore dimension of 3.1 nm that reasonably fits MB.[93] The maximum uptake capacity of MB was found to be 1691 mg g^{-1}. On the other hand, the microporous imine-linked triazine TS-COF-2 showed a maximum uptake capacity of 377 mg g^{-1} for the same dye, which is much lower than that for TS-COF-1. It confirms the relevance of suitable pore size for the uptake of dye pollutants. Moreover, the uptake of two larger dye molecules, RhB and Congo red (CR), was tested with TS-COF-1 and it was found that the maximum adsorption capacity is 625 and 319 mg g^{-1}, respectively. The retarded performance for the adsorption could be credited to the large size of the pollutants that are not well fit into the cavities of the adsorbent.

The chemo-selectivity and porosity of the adsorbent play a critical role in the separation of molecular dyes through targeted adsorption in water. A salicylideneaniline-based 2D-COF (SA-COF) formed by the Duff reaction exhibits reversible tautomerism in the presence of water molecules.[94] The *cis* and *trans*-keto forms of tautomerization in the solid-state COF are responsible for the dynamic changes in the ionic features of the pore walls which allows the selective ionic binding of the guest molecules. Under basic conditions, the positively charged molecules have interacted with the pore surface, whereas molecules are excluded from the surface under acidic conditions. These water-regulated functions in the SA-COF effectively separated the dye molecules based on their size, charge, and chemical nature. Three different dye molecules (MB, RhB, and chrome azurol S) were tested for size-selective separation by the SA-COF. The pore size of the SA-COF (1.45 nm) was slightly greater than that of the MB and RhB dye molecules, and less than the overall size of chrome azurol S. The effect of the molecular size on the adsorption was evident from the removal efficiency of each dye molecule. Notably, MB was rapidly adsorbed by the COF with a removal efficiency of 98.3% within 10 minutes. The slightly larger RhB was removed with an efficiency of 94.1% within 60 minutes, whereas the larger molecule chrome azurol S did not show notable adsorption due to the comparatively smaller size of the COF pores. Besides, the SA-COF displays charge selective adsorption both under acidic and basic conditions. The –OH and $–NH_2$ groups in the pore wall get deprotonated under basic conditions to become anionic. The *trans*-keto form of the SA-COF exhibited chemo-selectivity towards the molecules with the aromatic hydroxyl group instead of the aromatic amine group. It is evident from the higher affinity toward 1,4-hydroxyanthraquinone (90% removal efficiency within 60 min) compared to 1,4-diaminoanthraquinone (25% removal efficiency within 60 min).

The catalytic oxidation or reduction of toxic organic molecules is an alternative strategy for the decontamination of polluted water. Notably, a silver nanoparticle-loaded COF hybrid material showed a promising detoxification effect by catalytic reduction of aromatic nitro compounds into comparatively less toxic aromatic amines.[95] The 2D-COF (Ag@TPHH-COF) was composed of nitrogen and oxygen-rich building blocks 2,4,6-tris-(4-formylphenoxy)-1,3,5-triazine and hydrazine hydrate for preserving a stable dispersion of silver nanoparticles. The resulting Ag@TPHH-COF was also used for the catalytic hydrogenation of various organic dyes such as RhB, MB, MO, and CR.

The photocatalytic degradation of organic dyes is a type of advanced oxidation process for water treatment. In this chemical treatment, the photocatalyst effectively disintegrates the toxic molecular structure of dyes into a nontoxic version. COFs are well known for their π conjugated structure and semi-conductivity, which were effectively applied for the treatment of photocatalytic oxidation of organic dyes. For example, an AgI modified pyridine-connected β-ketoenamine COF was used to degrade RhB dye in water.[96] The improved separation of electron and hole pairs during the photocatalytic process enhanced the efficiency of the oxidation degradation process. RhB molecules were initially adsorbed on the COF/AgI composite and degraded by visible light irradiation within 80 minutes. Similarly, a metal-free β-ketoenamine TpBD COF was utilized for the photocatalytic degradation of various azo (N═N) dyes in water.[97]

Adaptive inclusion, an advanced concept of dye capture, was introduced in 2018 by taking the flexible reticular chemistry approach in which a novel isoreticular non-interpenetrated woven COF was constructed from aldehyde functionalized copper(I) bisphenanthroline complexes with benzidine linkers in the presence of a bulky anion, diphenylphosphinate ($PO_2Ph_2^-$).[98] Unlike the first-generation woven COF, COF-506-Cu possesses a flexible internal structure with guest accessible void space which promotes the dynamic motion of the frameworks. The incorporation of the bulky anion into the woven COF provided enough room in the internal voids. The metallated COF-506-Cu captures different fluorescent anionic dyes with decreasing efficiencies concerning the increasing molecular size of the dyes. However, compared to the metallated form, the demetallated COF-506 showed 11.6-fold higher uptake for larger dye molecules. The removal of metal from the COF enhanced the framework's flexibility in the intrinsic space of the COF and was capable of adsorb larger dye molecules. Although these works have been carried out in methanol solvent, we believe that the adaptive inclusion strategy can be extended to the potential remediation of water.

4.3 Removal of endocrine disrupting pollutants

Endocrine-disrupting chemicals (EDCs) are highly toxic pollutants that cause severe health risks including negative effects on the male and female reproductive system, causing cancer, and cardiovascular endocrinology.[99] EDCs are present in various plastic products used for food and drinking packages, plasticizers, pesticides, *etc.* Bisphenol A and bisphenol AF are two EDCs widely used to produce plastics and present in water at ppb level concentration. The efficient capture of bisphenol A and bisphenol AF was researched by controlling the uniform particle size of magnetic COFs. A monomer-mediated *in situ* growth strategy was adopted to control the uniform particle size of COFs.[100] In this method, the β-ketoenamine TpBD COF was fabricated on the surface of Fe_3O_4 magnetic nanospheres. The controlled growth of Fe_3O_4@TpBD core shells resulted in the formation of uniform spherical particles which showed moderate porosity (BET surface area of 272 $m^2\ g^{-1}$). The bisphenol A and bisphenol AF molecules were removed from the water with maximum adsorption capacities of 160.6 and 236.7 mg g^{-1}, respectively. Both pollutant molecules with π electron-rich aromatic benzene rings interacted with the π electron-rich 2D-layers of TpBD COF through π–π interactions. The photocatalytic degradation of BPA molecules was demonstrated by using a COF–MOF hybrid system.[101] The composite of β-ketoenamine COF and MOF (MIL-101-NH_2 or UiO-66-NH_2) photocatalytically degraded BPA molecules with 99% efficiency. The material enhanced the range of visible light absorption and effective separation of generated electron–hole pairs.

4.4 Removal of pharmaceutical micropollutants

Pharmaceutical compounds are composed of organic and inorganic molecules that are released/discharged to water sources in several ways.[102] Antibiotics are an important class of pharmaceutical compounds that are used for the treatment of bacterial infection in modern medicine. The uncontrolled deposition of antibiotics into the environment causes severe toxic pollution, especially for aquatic species. Recently, chemically stable polyarylether-based PEV-COFs were utilized for the extraction of antibiotic molecules from water.[55] Post-synthetically, acidic carboxylic acid (–COOH) and basic amino ($-NH_2$) groups were introduced to the pore walls of the COF. Three different tetracycline antibiotics (TCA – tetracycline, OTC – oxytetracycline, CTC – chlortetracycline hydrochloride) were removed from the aqueous solution by using these two chemically modified acidic and basic COFs. Notably, the antibiotics were efficiently removed from the water under acidic conditions by JUC-505-COOH (Q_{max}: TCA – 245.8 mg g^{-1}, OTC – 213.8 mg g^{-1}, and CTC – 238.9 mg g^{-1}) and under basic conditions by JUC-505-NH_2 (Q_{max}: TCA – 247.3 mg g^{-1}, OTC – 237.0 mg g^{-1}, and CTC –274.6 mg g^{-1}). The adsorption properties at various pH values of the solution depend on the functional group present in the framework. The adsorption is potentially due to the appropriate hydrogen bonding and electrostatic interactions between the antibiotics and functionalized COF. Diclofenac sodium, another pharmaceutical pollutant, was effectively

removed from water with a maximum adsorption capacity of 565 mg g^{-1} and removal efficiency of >97% by a magnetic β-ketoenamine COF (MCOF).[103] The COF was synthesized on the surface of $-NH_2$ functionalized magnetic nanoparticles (Fe_3O_4@SiO_2) through the salt-mediated crystallization method. The adsorption isotherm features rapid equilibrium within 20 min with the pseudo-second-order kinetic model (R^2 = 0.99).

4.5 Removal of disinfection byproducts

Chlorine (Cl_2) is one of the major disinfectants of drinking water, which causes the formation of toxic byproducts.[104] Halonitromethanes and trihalomethanes are highly carcinogenic, mutagenic, and teratogenic, and therefore, are highly recommended to be removed from drinking water. The COF-based remediation of disinfection byproducts from water using a nitrogen-rich 2D-COF (TpTt-COF) was introduced recently.[105] It was successfully utilized for the removal of bromodichloromethane (BDCM), nitrochloromethane (TCNM), dibromochloromethane (DBCM), and tribromomethane (TBM) through solid-phase extraction. The adsorption efficiency is highly efficient (~80–90%) at neutral pH. The hydrophobic nature of the COF resulted in an efficient interaction of the adsorbent and pollutant molecules. Besides, the hydroxyl functional groups present in the COF are believed to increase the polarity and enhance the extraction of disinfection byproduct molecules.

4.6 Removal of bromate

Bromate (BrO_3^-) is one of the major toxicities in drinking water that causes severe health risks such as depression, hemolytic anemia, and pulmonary edema, and is considered a possible human carcinogen.[106] The electrolysis and ozonolysis processes of water treatment of marine or freshwater are the major reasons for the contamination of bromate in drinking water. Many countries including those in the Middle East, Europe and the United States consume drinking water that is produced by such methods. The higher solubility and chemical stability of bromate in water signify potentially harmful effects for their long-term utilities. Moreover, BrO^{3-} ions are difficult to remove from water by using conventional water treatment methods. The induction of the Zincke reaction to construct a cationic porphyrin COF (PV-COF) with viologen linkers was reported for the effective removal of bromates from water. Notably, the quaternary ammonium salt linkage in this PV-COF induces the chemical stability of the framework in water. The cationic integrated framework with porphyrin units efficiently aids the weak interaction with bromate anions in water. The near mesoporous network with a uniform pore size (2.3 nm) allowed the lucid diffusion of the pollutant molecules into the porous matrix. An excellent uptake rate constant (191.45 g mg^{-1} min^{-1}) and remarkable uptake capacity (203.8 mg g^{-1}) were observed. The PV-COF could reduce the bromate concentration in water from 50 μgL^{-1} to lower than the safe limit of 3 μg L^{-1} within 20 minutes. The excellent removal efficiency (95%) indicated the favorable electrostatic interaction of the PV-COF with bromate ions. The kinetic adsorption analysis provided the efficiency of the PV-COF compared to other BrO_3^- sorbents. The pseudo-second-order kinetic adsorption isotherm estimated an adsorption rate of 191.45 g mg^{-1} min^{-1}, whereas a maximum adsorption capacity of 203.8 mg g^{-1} was found from the Langmuir model. Moreover, the adsorption efficiencies were maintained for 3 cycles of analysis.

4.7 Removal of organophosphate flame retardants

Organophosphate flame retardants (OPFRs) are one of the important organic chemicals for the prevention of ignition and flame retardants in varnishes, plastics, electronic equipment, and other materials. In the last few years, studies show that the heavy use of such chemicals in popular materials causes large bioaccumulation and severe environmental impact.[107] Triphenyl phosphate (TPhP) is a widely used OPER that accumulates in water bodies and in drinking water. The presence of TPhP molecules in water causes a threat to the well-being of aqua and non-aqua living species.[108] The reticular porous feature of COFs was explored for the uptake of TPhP in water. Three different β-ketoenamine COFs consisting of various lengths of C_2 linkers such as *p*-phenyl diamine (one benzene ring), benzidine (two benzene rings), and terphenyl (three benzene rings) with controlled 1D nanochannels were used for TPhP adsorption.[109] The benzidine-linked TpBD-COF with a pore diameter of 2.57 nm showed a maximum adsorption capacity of 387 mg g^{-1} compared to the TpPa-1 COF (86.1 mg g^{-1}) and TpTer COF (371 mg g^{-1}) with pore sizes of 1.81 and 3.34 nm, respectively. The smaller pore size of the TpPa-1 COF blocks TPhP into the porous matrix; hence the adsorption efficiency was reduced significantly. On the other hand, the large pore size of the TpTer-COF effectively decreased the sorption energy which has been calculated from the DFT analysis.

4.8 Removal of marine biotoxins

Marine biotoxins are toxic pollutants generated from aquatic species. Diarrhetic shellfish poison (DSP) is one important type of marine biotoxin which poisons aquatic drinking water and causes intense diarrhea and severe abdominal pains.[110] Acidic toxins like okadaic acid and its derivative dinophysistoxin-1 are highly toxic molecular pollutants originating from DSP. A magnetic β-ketoenamine COF (*o*-toluidine as a C_2 linker) was successfully applied for the removal of both okadaic acid and dinophysistoxin-1 from marine water.[111] The MCOF extracted okadaic acid with a maximum adsorption capacity of 812 mg g^{-1} and dinophysistoxin-1 with a maximum adsorption capacity of 530 mg g^{-1}. The removal efficiency is much better compared to commonly used macroporous resins. The extracted marine biotoxins were completely desorbed from the MCOF and the adsorbent was repeatedly used for four cycles.

4.9 Removal of toxic heavy metals

In addition to organic micropollutants, heavy metals are another major class of toxic agents in water. Heavy metals are generally known for their toxicity both for aqua and non-aqua living species. Their presence in water even at very low concentration (at the ppb level) results in high toxicity.[112,113] The maximum permissible concentration of most hazardous heavy metals such as mercury, lead, cadmium, arsenic, and chromium is limited in microgram per liter scale in drinking water.[114] The ionic forms of these heavy metals are highly soluble in water, which increases the mobility of these metal ions that helps their rapid spread in water bodies. The heavy metals are discharged into freshwater reservoirs through various sources including industries, urban areas, mining, agriculture, and wastewater treatment plants. The consumption of polluted water and aqua-living species causes bioaccumulation of toxic metals. In this regard, the ultra-purification of toxic metal-polluted water before discharging into the reservoirs is required for a healthy living society. The advanced chemistry offers the specific binding of such heavy metals into the functional sites of the porous materials through hard and soft acid–base (HSAB) interactions (Fig. 6a). The soft–soft interaction of mercury (Hg) and sulfur (S) was explored for the sensing and removal of Hg^{2+} ions from water by using a thioether integrated 2D-COF.[115] The thioether grafted hydrazone-linked COF-LZU8 was designed and synthesized by using the organic building blocks 2,5-bis(3-ethylthio)propoxy)terephthalohydrazide and 1,3,5-triformylbenzene (Fig. 6b). The specific binding of Hg^{2+} ions among a mixture of metal ions by COF-LZU8 indicated highly desired selective adsorption properties. The selective removal of Hg^{2+} from water and the recyclable use of COF-LZU8 signified the potential practical application of the COF. It showed a removal efficiency of 98% at a low concentration of Hg^{2+} ions (0.2 ppm) with excellent recyclability over three cycles.

The functional and porosity modification of 2D-COFs enhanced the uptake efficiency of Hg^{2+} ions from water. Two independent approaches were introduced in 2017 for the improved capture of Hg^{2+} ions from water by using 1,3,5-tris(4-aminophenyl)-benzene as a C_3 knot in the imine-linked 2D-framework of COFs (Fig. 6c). In one strategy, researchers post synthetically modified a vinyl functionalized COF into a 'thioether and thiol' carrying porous matrix using the thio–enol click reaction.[116] The vinyl decorated COF (COF-V) was constructed by the imine condensation between 2,5-divinylterephthalaldehyde and 1,3,5-tris(4-aminophenyl)-benzene. The mesoporous COF-S-SH (pore diameter of 2.8 nm, BET surface area of 546 $m^2\ g^{-1}$) strongly interacted with Hg^{2+}ions, which was evident from the steep adsorption in the type 1 isotherm profile. The kinetic analysis showed the adsorption affinity of the thiol functionality integrated COF towards Hg^{2+} ions. The large number of highly accessible sulfur groups in the ordered mesopores of COF-S-SH could interact with Hg^{2+} ions and purify the water from 5 ppm into 0.73 ppb concentration of Hg^{2+} (removal efficiency: 99%.) within 10 minutes. The treatment of COF-S-SH with 1,2-ethanedithiol solvent regenerated the Hg^{2+} ion free COF which was reused for three cycles with an adsorption capacity of ~1280 mg g^{-1}. In another strategy, researchers reported a large pore structure (3.2 nm) imine-linked 2D-COF (from monomers 1,3,5-tris(4-aminophenyl)benzene (TAPB) and 2,5-bis(methylthio)terephthalaldehyde (DMTTPA)) with short-chain thioether groups at the pore walls (Fig. 6c).[117] The COF is extremely stable in a wide pH range due to the integration of the resonance effect in the phenyl edges. The reticular design of the large pore aperture with a high BET surface area (1934 $m^2\ g^{-1}$) of the COF boosted the heavy metal ion diffusion through the entire porous matrix with enhanced functional accessibility. It was noted that the chemical stability of the thioether group is higher than the thiol group towards oxygen oxidation. Considering these facts, an excellent removal of Hg^{2+} ions from water was observed for the TAPB–BMTTPA-COF with a calculated saturated removal capacity of 734 mg g^{-1}. It showed that a larger portion (76%) of integrated methyl sulfides was exposed for the Hg^{2+} ion adsorption. The kinetic study suggested rapid removal of Hg^{2+} ions (99% of Hg^{2+} ions were removed within 5 min) from water. Moreover, the TAPBBMTTPA-COF showed a good performance over a wide range of pH (0 to 14) and maintained a removal efficiency of 92% even after six cycles. The regeneration of the structurally intact TAPBBMTTPA-COF was achieved by treatment with 6 M HCl, which results in 100% demetallation. The selective affinity of the TAPBBMTTPA-COF towards toxic heavy metal ions like Hg^{2+} and Pb^{2+} ions compared to other metal ions such as Zn^{2+}, Fe^{3+}, Mg^{2+}, Ca^{2+}, and K^+ indicates the potential benefits of the COF adsorbent.

The removal of Hg^{2+} ions from water was also carried out through extraction by a magnetic β-ketoenamine COF.[118] The hetero-linked (4,4′-diaminodiphenyldisulfide and *p*-azoaniline as C_2 linkers and 1,3,5-triformylphloroglucinol as a C_3 knot) MCOF was fabricated and further modified into a thiol functionalized MCOF. The disulfide linkages in the framework were chemically converted to thiol functional groups by using the bond-breaking strategy with tributylphosphine acid. MCOF-SH takes up Hg^{2+} ions from water with a maximum adsorption capacity of 383 mg g^{-1}. The electronegative nitrogen and oxygen atoms in the hydrazone pocket in a 2D-COF strongly bind Hg^{2+} ions from water through electrostatic and coordination interactions.[119] The hydrazone pocket contains –C═O and secondary –NH– groups which can effectively chelate with the heavy metal ions. The hydrazone-linked β-ketoenamine TpDOH COF (constructed from flexible alkyl amine oxalyldihydrazide as a C_2 linker) largely improved the maximum adsorption capacity of Hg^{2+} ions (1692 mg g^{-1}). Similarly, the Cu^{2+} ions were also removed from water with a maximum uptake of 324 mg g^{-1}.

Arsenic is another toxic heavy metal pollutant present in groundwater in its As^{3+} and As^{5+} ionic states. The arsenic bioaccumulation in living bodies results in several health

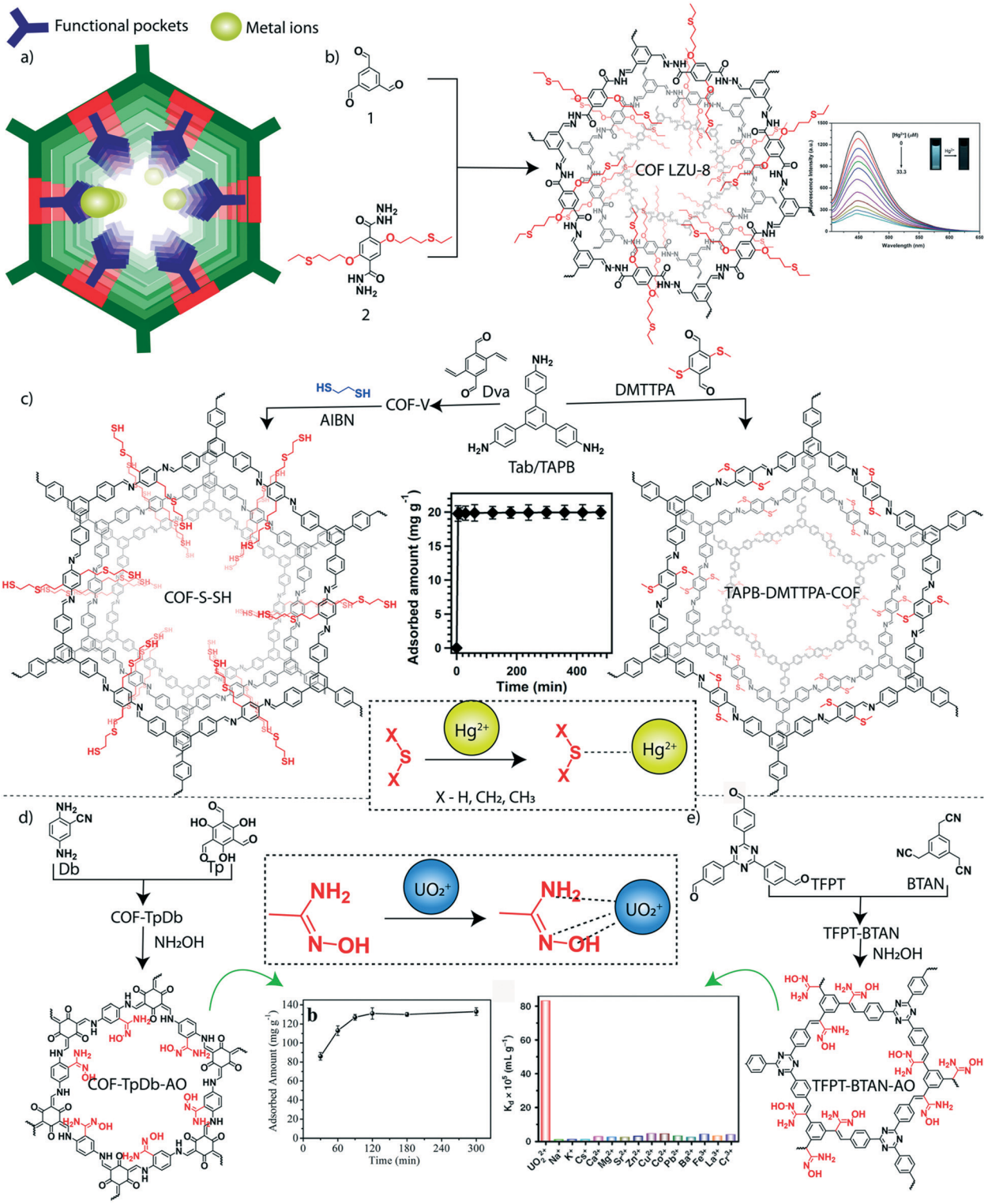

Fig. 6 Granular COFs for inorganic micropollutant removal from water. a) The diagrammatic representation of metal adsorption sites in the COF. b) The schematic representation of the synthesis of predesigned thioether integrated COF-LZU-8. c) The post-synthetic modification of the 1,3,5-tris(4-aminophenyl)benzene (C_3) connected COF into COF-S-SH and TAPB–DMTTPA-COF. d) The schematic representation of amidoxime functionalized (through post-synthetic modification) β-ketoenamine COF-TpDb–AO and the uranium capture efficiency plot. e) The schematic representation of amidoxime functionalized (through post-synthetic modification) conjugated TFPT–BTAN–AO and the selective uranium capture efficiency plot. [Reproduced from ref. 88 (Fig. 6b data) and ref. 90 (Fig. 6c data) with permission from American Chemical Society, Copyright 2016 and Copyright 2017. Reproduced from ref. 99 (Fig. 6d data) with permission from John Wiley and Sons, copyright 2018. Reproduced from ref. 100 (Fig. 6e data) with permission from Springer Nature, copyright 2020].

problems including skin lesions, cardiovascular diseases, diabetes, and even cancer.[120] Several purification strategies including filtration, iron oxide and activated alumina adsorption, ion exchange, reverse osmosis, and electrodialysis are adopted to remove arsenic from water. In a recent investigation, researchers successfully applied an ethidium bromide-linked cationic framework, *i.e.*, EB-COF:Br for the effective removal of As^{5+} from water.[121] The arsenic ions are freely transported through the uniformly distributed micropores (pore size: 1.7 nm) and trapped into orderly placed cationic linkers. The maximum adsorption capacity in neutral water was found to be 53.1, 27.5, and 5.1 mg g^{-1} at 25 °C, 35 °C, and 45 °C, respectively. The exothermic nature of the COF···As interaction was revealed from a steady decrease in the adsorption capacity with an increase in temperature. Moreover, the COF···As interaction is stronger than the interaction of the metal with water molecules. The maximum adsorption capacity of As^{5+} ions from contaminated river water was found to be 8.2 mg g^{-1} at 25 °C. In another study, the β-ketoenamine TpPa-1 magnetic COF was employed for the removal of toxic Cr^{6+} ions from water.[122] The adsorption of Cr^{6+} ions with the porous adsorbent depends on the pH of the aqueous solution with removal efficiencies of 90%, 60%, and 30% at pH 1, 2, and 3 respectively. The maximum adsorption capacities of Cr^{6+} ions were calculated to be 310.8 mg g^{-1} and 245.45 mg g^{-1} for pristine TpPa-1 COF and magnetic Fe_3O_4@TpPa-1, respectively.

The post-synthetic modification of pore walls in the β-ketoenamine $TpPa(NO_2)_2$ COF with ethylenediaminetetraacetic acid (EDTA) facilitates the broad uptake of various heavy metal ions including soft Lewis acids (Ag^+, Pd^{2+}), hard Lewis acids (Fe^{3+}, Cr^{3+}), and borderline Lewis acids (Cu^{2+}, Ni^{2+}).[123] The strong metal chelating ability of EDTA through their electronegative oxygen and nitrogen atoms enhanced the uptake of metal ions. The EDTA functionalized COF displayed a removal efficiency of 85% within 5 minutes. The adsorption capacity was high at pH ≥ 3 and decreased along with lower pH due to the competitive interaction of H^+ ions. The maximum adsorption capacities (above 50 mg g^{-1}) of the tested metal ions were observed at a relatively high concentration (100 ppm) of the solution plausibly because of favorable chelation.

4.10 Removal of radio-active pollutants

Although nuclear power is a major alternative energy source for fossil fuels, the possible toxic contamination by nuclear waste is a serious threat to the environment. The uranium leakage from the nuclear power industry can be very dangerous to the living system; therefore, the detection and separation of uranium from water sources are very important. Amidoximes are well-known functional pockets for chelating UO^{2+} ions through the two nitrogen and one oxygen in the chain.[124,125] Amidoximes were chemically grafted into the porous matrix of a COF as a potential uranium extractor.[126] The first attempt was carried out in the β-ketoenamine TpDb COF (synthesized from 2,5-diaminobenzonitrile (Db) with triformylphloroglucinol (Tp)) to modify the framework with amidoxime functional moieties (COF-TpDb-AO) (Fig. 6d). The BET surface area of COF-TpDb (1164 m^2 g^{-1}) was maintained even after the chemical modification (COF-TpDb-AO – 864 m^2 g^{-1}). The saturation adsorption capacity was calculated to be 408 mg g^{-1} in the initial uranium concentration range of 23.1–265.2 ppm. The rapid adsorption of uranium ions (removal efficiency of 95% within 30 minutes) and reusability over three cycles indicated the potential use of the amidoxime modified COF. The comparison of the adsorption kinetics of the crystalline COF with the corresponding amorphous polymer clearly showed the advantages of the ordered porosity for rapid adsorption. The immediate contact of pollutant molecules leads to a higher adsorption rate (95% removal within 30 minutes for the COF, whereas the amorphous version took 90 minutes to reach the same efficiency).

A similar post-modification strategy was employed for the synthesis of the sp^2 carbon-conjugated fluorescent TFPT-BTAN-AO COF with chemical, thermal, and radiation stability.[127] The COF not only adsorbs uranium but also functions as a uranium sensor in water even at a lower concentration. The synthetic scheme of the TFPT-BTAN COF involves the construction of a triazine framework from 2,4,6-tris(4-formylphenyl)-1,3,5-triazine (TFPT) and 2,2′,2″-(benzene-1,3,5-triyl)triacetonitrile (BTAN) through the Knoevenagel polymerization reaction (Fig. 6e). Consequently, the cyano-based TFPT-BTAN COF was chemically functionalized with the amidoxime group. The strong blue fluorescence of TFPT-BTAN-AO was selectively quenched by the UO^{2+} ions in the aqueous solution due to the interaction of UO^{2+} with the amidoxime functional groups. Therefore, the presence of UO^{2+} ions was detected even at an ultra-low concentration (6.7 nM) in water within 2 seconds. The specific interaction of amidoxime with UO^{2+} ions facilitated the selective sensing of radioactive UO^{2+} ions from a mixture of metal ions in water. The targeted binding of UO^{2+} ions by the TFPT-BTAN-AO COF results in an excellent uptake capacity of 427 mg g^{-1}. The open porous structure of the COF allowed 68% of the amidoxime functional groups to be exposed and interacted with the UO^{2+} ions. The rapid saturation capacity (98% within 45 minutes) and recyclability over six cycles with 95% removal efficiency demonstrated the great potential of the COF for radionuclide detection and extraction. Similarly, the amidoxime decorated sp^2 carbon-conjugated fluorescent COF-PDAN-AO (constructed from the monomers 1,3,6,8-tetrakis(4-formylphenyl)pyrene and 1,4-phenylenediacetonitrile) was also reported for the ultra-low detection (6.5 nM) and efficient adsorption (410 mg g^{-1}) of uranium from radioactive wastewater.[128] Meanwhile, marine biofouling is one of the critical challenges to overcome for long-lasting uranium extraction from seawater. The marine biospecies can be accumulated in the porous surface of the adsorbent and reduce the efficiency of uranium recovery. To address this challenge, a series of amidoxime functionalized

olefin-linked COFs were demonstrated for their anti-biofouling activities and subsequently enhanced enrichment of uranium adsorption. The triazine and alkynyl moieties with the olefin-linked frameworks promote photocatalytically induced reactive oxygen species (ROS) which act as an anti-biofoulingagent.[129,130] Besides, the photoelectric effect induced the reduction of U(VI) to insoluble U(IV) which increased the recovery of the ions. The solar light-induced uranium extraction uptake is 1.42–1.48 times higher than the extraction without light. A similar photoactive strategy has also been extended to a hydrophilic benzoxazole-based COF for selective uranium uptake.[131] The hydroxyl groups present in Tp and the benzoxazole ring effectively improved the affinity of the network toward uranyl ions.

The post-functionalized carboxyl group (–COOH) integrated 3D-COF was demonstrated for its higher affinity towards radio-active Nd^{3+} ion extraction from water.[132] The 3D-COF was synthesized from tetra(4-formylphenyl) methane as a tetrahedral building unit and 3,3′-dihydroxybenzidine (DHBD) as a linear C_2 linker carrying hydroxyl groups (OH). The hydroxyl groups were treated with succinic anhydride to form a –COOH functional chain at the pore walls of the 3D-COF. The presence of the –COOH group in the open microporous (0.68 nm) 3D framework allowed the extraction of various metal ions, especially radio-active Nd^{3+} ions from water. It was found that the uptake amount of Nd^{3+} ions was higher than that of Sr^{2+} and Fe^{3+} ions. The greater charge density of Nd^{3+} compared to the other two metal ions could be the possible reason for the tight binding with the –COOH functional pockets in the 3D framework. Particularly, the ideal adsorbed solution theory (IAST) showed that the 3D-COOH-COF preferred Nd^{3+} ions from the solution of a mixture of 5% Nd^{3+} and 95% Fe^{3+} or Sr^{2+}. 27% of the Nd^{3+} ions were removed from this solution mixture, whereas only 18% of Fe^{3+} ions were removed which indicates the selective extraction of Nd^{3+} from a mixture of metal ions.

5. COF membranes for water purification

5.1 Current strategies to fabricate COF membranes

The commercial level water treatment involves the separation of pollutants through selective barrier membranes. The membrane-based technology is beneficial due to its cost-effective nature, minimal use of energy, and continuous operation features. The industrially important membranes are made up of amorphous porous polymers for the removal of various contaminations from water.[133] However, the separation of micropollutants from water required micro and mesoporous membranes without any large defects. The use of such ultra nanoporous amorphous polymeric membranes reduces the solvent flux due to the haphazard distribution of the pores without any uniform size. The amorphous pore distribution blocks the transportation of water molecules and creates heavy pressure on the membrane. The nanofiltration membrane prefers to be the uniform micro or mesoporous platform with regular arrangement of pores. The ordered specific porosity features allow the better flow of water with the selective rejection of micropollutants based on their size.

Considering their inherent properties, COFs are the ideal platform for inducing ordered porosity with desired size and shape into a membrane matrix. In 2016, the chemically stable β-ketoenamine TpPa-2 COF was fabricated into a mixed matrix membrane with a polysulfone porous support and applied for the separation of 90% of humic acid from water.[134] The nanofiltration ability of an interfacial polymerized imine-linked 2D-COF on a porous polymer support (polyethersulfone) was demonstrated in 2017.[135] In this thin-film composite, the mesoporous TAPB–PDA COF (pore size ~3.4 nm) acted as an active-layer for the separation of rhodamine-WT from water.

However, these COF composites were applied with the mechanical support of another porous matrix for separation application. The external porous agent mechanically supports the non-free-standing COF thin film but may hinder the diffusion of water molecules. In this regard, the COF should be fabricated as a free-standing membrane without any external mechanical assistance. But the crystalline particles of COFs made it difficult for them to assemble into 2D-macroscopic forms. The conventional solvothermal synthesis of COFs often provides a highly granular nature of the material.

The above-mentioned challenges were effectively addressed in the pioneering work of the salt-mediated solid-state synthesis of free-standing β-ketoenamine COF membranes (COMs).[44] The crystalline β-ketoenamine frameworks were formed from various aromatic diamine linkers and 1,3,5-triformylphloroglucinol through *p*-toluenesulphonic acid-mediated catalysis in the mechanochemical solid-state synthesis (Fig. 7a and d). The amine···PTSA organic salts were reacted with aldehyde with reduced kinetics offering regular formation of the frameworks in the solid-state reactant mixture. Moreover, the paste form of the reactant mixture allowed the fabrication of thick stand-alone membranes (200–300 μm thickness) through the knife-casting technology. The porous and crystalline free-standing COF membranes have a mechanically strong and continuous crack-free structure.

However, the large membrane thickness of these solid-state synthesized COF membranes (200–300 μm) partially reduces the flow rate of water through the internal pores. On this ground, the interfacial polymerization of porous and crystalline β-ketoenamine COFs in 2D-thin film architecture was introduced for the high flow rate and effective removal of organic micropollutants from water.[72] The bottom-up interfacial crystallization strategy was used to fabricate a large area (in centimeter-scale) of COF film membranes with nanometer-level thickness (~50–90 nm) at room temperature devoid of any additional supply of energy (Fig. 7c). The COF thin film was grown at the interface of water–dichloromethane solvents. The symmetric aromatic amine building units were solvated in the form of PTSA–amine salt in water and a C_3

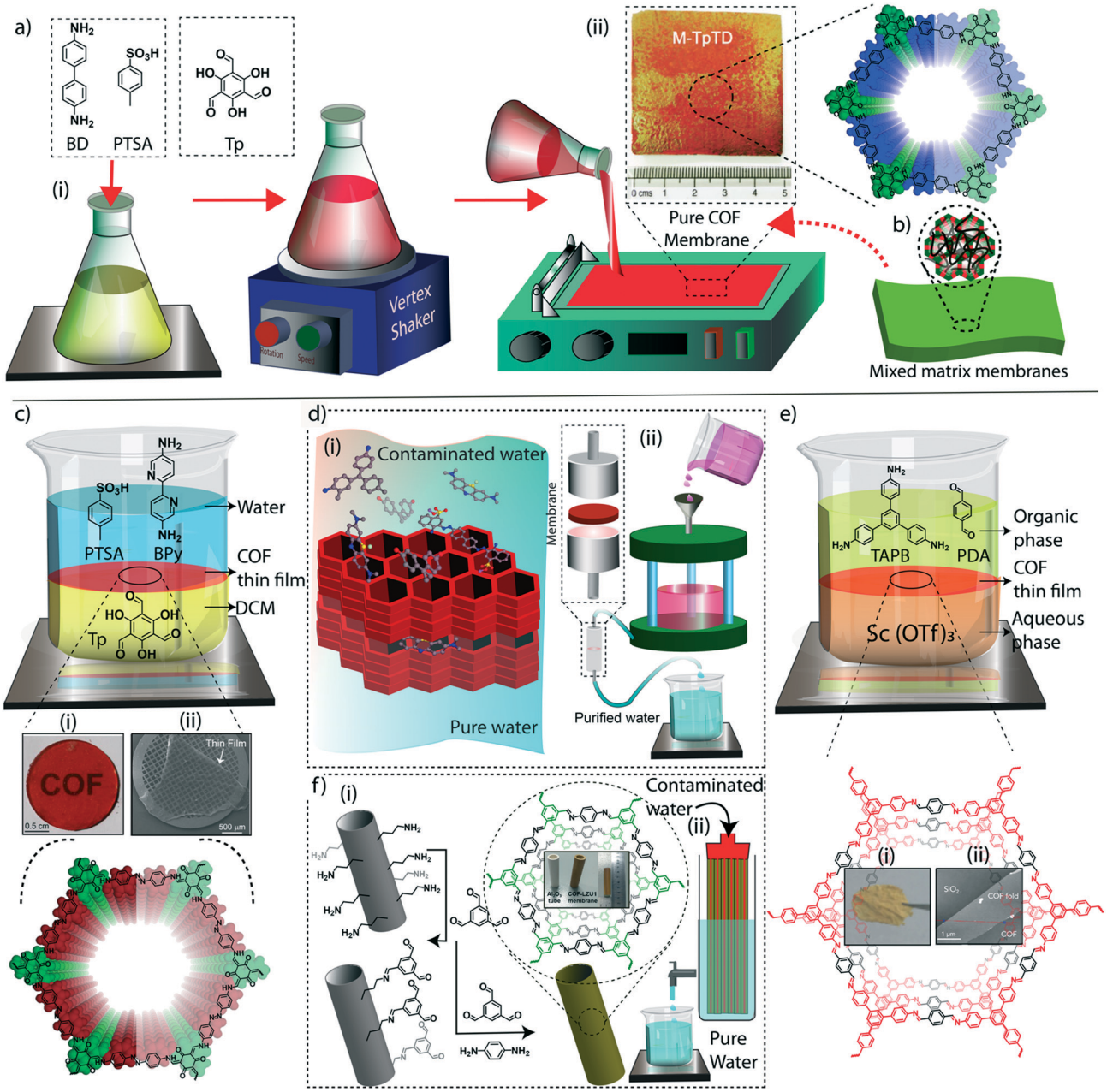

Fig. 7 COF membranes for water treatment. a) The diagrammatic representation of COF membrane synthesis: (i) mechano-mixing of PTSA and amine linker followed by the addition of Tp, (ii) membrane casting into different areas and thickness. b) The diagrammatic representation of the mixed matrix membrane. c) The diagrammatic representation of the interfacial synthesis of β-ketoenamine COF thin film with (i) digital and (ii) SEM images. d) (i) and (ii) The COF membrane-based water purification. e) The diagrammatic representation of the interfacial synthesis of imine COF thin film with (i) digital and (ii) SEM images. f) (i) The imine-linked COF-LZU thin-film coated tubular membrane, (ii) tubular membrane-based water purification. [Reproduced from ref. 44 (Fig. 7aii) with permission from John Wiley and Sons, copyright 2016. Reproduced from ref. 72 (Fig. 7ci and ii) with permission from American Chemical Society, Copyright 2017. Reproduced from ref. 73 (Fig. 7ei and ii) with permission from Elsevier, Copyright 2018. Reproduced from ref. 70 (Fig. 7f photograph) with permission from John Wiley and Sons, Copyright 2018].

aldehyde knot (1,3,5-triformylpholoroglucinol) was dissolved in dichloromethane. This design principle allowed simultaneous control over the crystallization and morphology of the framework structure with permanent ordered porosity (Tp–Bpy COF shows the highest BET surface area, 1151 $m^2\ g^{-1}$). The intermolecular hydrogen bonding between the amine and PTSA effectively reduced the strength of the nucleophilicity of amine linkers and controlled the rapid diffusion rate of the monomers into the interface of the bilayer system. The resulting slow reaction kinetics and diffusion rate create a thermodynamic control over the reaction which led to regular framework formation with π–π interaction. These COF thin films were easily transferrable into different supports including loops and porous support membranes.

The imine-linked COF thin films were deposited on a porous alumina support with a thickness of 100–300 nm for the hollow-tubular membrane-based separation of organic dyes from water (Fig. 7f). Unlike 2D membrane separation, the hollow tube membrane water treatment follows the long 1D-occupied contaminated water in the tube that is filtered to the surrounding of the membrane. In this regard, the hydrothermally stable COF-LZU1 was demonstrated for hollow tube membrane water filtration.[70] The COF was synthesized from the imine condensation of 1,3,5-triformylbenzene (TFB) and *p*-phenylenediamine (PDA) on the surface of chemically modified porous alumina (TFB was treated with amino-Al_2O_3). The solid surface interfacial polymerization offers COF-LZU1 porous, thin-film coating on Al_2O_3 in sub 500 nm thickness.

5.2 Removal of organic pollutants

The PTSA mediated solid-state synthesized COMs rejected organic dyes such as rose bengal (99%), methylene blue (94%), and Congo red (96%) from water with excellent removal efficiencies.[44] The mechanism of dye removal was demonstrated as a molecular sieving effect through the nanochannels of COMs. The COMs were also applicable for the effective removal of important active pharmaceutical ingredient vitamin B12 (V-B12; MW: 1344; ≈1.7 nm × 1.8 nm) from water. The M-TpBD and M-TpTD COMs rejected vitamin B12 with removal efficiencies over 95%. Another pharmaceutical ingredient, tetracycline, was rejected by M-TpBD with an efficiency of 81%. Also, the COM removed toxic Gram-negative *Escherichia coli* from water. Moreover, the chemical stability of the COF membranes is of paramount importance in commercial level separation applications. The chemical fragility of imine-inked COFs towards harsh acidic and basic environments suppresses their opportunities in potential membrane-based separations. The introduction of the methoxy group (2,4,6- trimethoxy-1,3,5-benzenetricarbaldehyde [TpOMe]) into the frameworks through the solid-state synthesis overcomes the chemical stability problems of the imine-linked COFs.[54] The solid-state mixing strategy offered the fabrication of six different COFs suitable for the separation of various pollutants from water without any additional support. The remarkable flux rate (117.6 L m^{-2} h^{-1} bar^{-1}) of water through the COMs is due to the ordered porosity of the membrane. The molecular sieving of the potent organic dyes through the controlled intrinsic pores in the COMs allowed the size-selective separation of various pollutants from water. Notably, rose bengal (RB; molecular weight: 1017.6; dimension of ≈1.2 nm × 1.54 nm), MB (molecular weight: 319.8; ≈0.75 nm × 1.52 nm), and CR (molecular weight: 696.6; ≈0.75 nm × 1.9 nm) organic dyes were rejected by the M-TpBD membrane (pore size 2.1 nm) with efficiencies of 99%, 94%, and 96%, respectively. Notably, the rejection efficiencies were changed for RB (84%), MB (83%), and CR (80%) when the intrinsic pore size was extended to 2.6 nm in the M-TpTD COF membrane. This size-selective molecular sieving was further investigated for the mixture of two different sized organic dyes (rose bengal and nitroaniline (molecular weight: 138; ≈0.44 nm × 0.7 nm)) in water. The COM allowed only nitroaniline molecules to pass through the pores and rejected larger-sized rose bengal molecules. Whereas the ultra chemically stable TpOMe based imine-linked COF membranes were used to separate highly acidic solutions. The aq. H_2SO_4 solution (0.5 M, 1.5 M, 3 M, and 6 M) was permeated through these membranes without any decomposition of the porous framework due to the chemical inertness towards acidic conditions. Moreover, the COF membranes were used for the molecular separation of toxic organic dyes from water showing high removal efficiency (>99%) and good recyclability.

The bilayer interfacial synthesized β-ketoenamine 2D-COFs were reported for their improved solvent flux in the membrane-based separation process.[72] As a result of the reduced thickness of the membrane, the water permeation (211 L m^{-2} h^{-1} bar^{-1}) value of the Tp–Bpy COF thin film was found to be larger than those for polyamide-based nanofiltration membranes. Again, the Tp–Bpy COF thin-film performed the separation of organic dyes with rejection efficiencies as high as 94% (brilliant blue-G (BB)), 80% (CR), 97% (acid fuchsin (AF)), and 98% (RhB); meanwhile, those for Tp–Azo are 90% (BB), 79% (CR), 99% (AF), and 99% (RhB). The large acid fuchsin molecules were size-selectively rejected by the thin-film membrane from the mixed feed of acid fuchsin [molecular weight = 585.5; ~1.19 nm × 1.14 nm] and *p*-nitrophenol [molecular weight = 139.1; ~0.66 nm × 0.43 nm] in water. Moreover, the COF thin-film membrane was highly recyclable for at least five cycles. The interfacial synthesis of the β-ketoenamine COF was further extended to the fabrication of the cationic ethidium bromide linked EB-COF:Br thin-film membrane (thickness of 155–165 nm) with an improved flux rate of water (546 L m^{-2} h^{-1} bar^{-1}) for charge-selective molecular separation.[136] The cationic framework could effectively separate anionic pollutants such as MO (99.6%), fluorescein sodium salt (99.2%), and potassium permanganate (98.1%) from water compared to neutral dyes (Nile red (22.3%), calcein (74.4%), and *p*-nitroaniline (15.7%)) and cationic dyes (RhB (91.2%), MB (87.2%) and *N*,*N*-dimethyl-*p*-phenylenediamine dihydrochloride (84.9%)). Principally, the anionic guest molecules have electrostatically interacted with the cationic pore surface of the EB-COF:Br thin film membrane. As a result, it could block further passage of anionic dyes and allowed only the movement of the solvent, whereas the cationic dyes were rejected due to the electrostatic repulsion between similarly charged pore walls and dyes. Meanwhile, the neutral dyes were rejected through size-selective molecular sieving through the thin film membrane.

In 2018, the interfacial synthesis of an imine-linked COF thin-film membrane for organic dye molecular separation was reported.[73] The imine networks of the COF thin film

were formed from 1,3,5-tris(4-aminophenyl)benzene (TAPB) and terephthaldehyde (PDA) at the interface of the organic and aqueous solvent system. The building molecules were present in the organic phase and the Lewis acid catalyst $Sc(OTf)_3$ was dissolved in the aqueous phase (Fig. 7e). The COF thin film with polyethersulfone rejected rhodamine dye from water with a removal efficiency of 91%, which is better than that for the polyethersulfone membrane alone.

The interfacial synthesis often provides the AA stacking of COF layers which is attributed to the maximum possible pore aperture for the COF membranes. The manipulation of the functional moieties of the monomers of the COF thin films effectively reduced the pore size from >1 nm to the sub-nm scale through the alternative AB stacking of the 2D layers.[137] Interfacial polymerization involving two miscible organic solvents that are separated by a low-density solvent as a buffer interlayer was reported. Two different COF membranes were fabricated from 1,3,5-triformylphloroglucinol (TFP) or 2,4,6-triformylphenol (Sa) as a C_3 knot with the common C_3 linker tris(4-aminophenyl)amine (TAPA) monomers. The pore aperture sizes of these COF membranes were controlled by the number of hydroxyl groups (OH) present in the C_3 knot. The higher numbers of hydroxyl groups in TFP promoted the formation of AB stacked layers with a pore aperture size of 0.6 nm (FS-COM-1), whereas only one hydroxyl group in the knot resulted in the AA stacked COF with a pore size of 0.95 nm (FS-COM-2). The flux rate of water (~38.6 L m^{-2} h^{-1} MPa^{-1}) was reduced due to the sub-nanometer porosity of the membrane. However, FS-COM-1 efficiently rejected fourteen different cations and RhB molecules from water. Moreover, Na_2SO_4 and K_2SO_4 have been removed from water with 90% and 95% efficiencies, respectively.

The interfacially deposited COF-LZU1 thin-film on alumina tube was explored for hollow tube-based water filtration.[52] The remarkable flux of water (390 L m^{-2} h^{-1} MPa^{-1} and even reached up to 760 L m^{-2} h^{-1} MPa^{-1}) for COF LZU 1 coated porous alumina is higher than those of commercial nanofiltration membranes (typically in the range of 10–50 L m^{-2} h^{-1} MPa^{-1}). The microporous (pore diameter 1.8 nm) COF thin film coated on porous alumina effectively separated several organic dyes from water with high rejection efficiencies: 1) MB (99.2%), 2) CR (98.6%), 3) black T (98.2%), 4) RB (99.1%) and AF (91.4%).

In another study, exfoliated β-ketoenamine COF nanosheets were fabricated into the membrane on an anodic aluminum substrate for the separation of organic dyes from water.[138] The β-ketoenamine COFs were synthesized in the presence of azobenzene and they were exfoliated into nanosheets upon irradiation with 365 nm UV light. The *trans*-form of the azobenzene in the interlayer space of the COF is converted into the *cis*-form that breaks the internal interaction between the 2D layers. The fabricated Tp-AD-50 membrane rejected several organic dyes including direct red 80 (98.5%), CR (82%), RB (98%), and methyl violet (MV; 88.3%) with flux-rates of 459 L m^{-2} h^{-1} MPa^{-1}, 491 L m^{-2} h^{-1} MPa^{-1}, 541 L m^{-2} h^{-1} MPa^{-1}, 551 L m^{-2} h^{-1} MPa^{-1}, and 593 L m^{-2} h^{-1} MPa^{-1}, respectively.

In addition to the control over porosity, chemical functionalization also plays a key role in improving the flux rate of water and the selective removal of pollutants. The hydrophilicity of the 2D-membrane has been enhanced through the mixed dimensional approach to fabricate a composite membrane from a cationic guanidinium-linked β-ketoenamine TpTGCl COF (as 2D component) and negatively charged TEMPO-oxidized CNFs with a high density of –COOH groups (as 1D component).[139] This interlamellar microporous network was supported on a polyacrylonitrile (PAN) substrate and showed robust mechanical tensile strength (108.3 MPa) and elastic modulus up to 3.62 GPa. The numerous –COOH functional groups in the membrane increased the hydrophilicity (the water contact angle of 7.2° was decreased to ~0° within only 0.2 s) which affects the separation of water from alcohol. The C_2–C_4 alcohols were readily rejected by the TpTGCl@CNFs-5/PAN membrane and water permeation was over 99.5 wt% with the separation factor (αwater/alcohol) higher than 2000 (3876 for *n*-butanol dehydration). The microporous COF–CNF composite membrane also size-selectively removed organic dyes such as CR (99.6%), alcian blue (98.3%), MB (90.3%), and orange GII (90.3%) with permeance higher than 70 L m^{-2} h^{-1} MPa^{-1}. The hydrophilic microporous (0.65 nm) TpTGCl@CNFs-4/PAN membrane also rejected Na_2SO_4 from water with a removal efficiency of 96.8% and permeance of 42.8 L m^{-2} h^{-1} MPa^{-1}.

5.3 Removal of tetraalkyl ammonium salts

A mechanically robust carboxylic acid (–COOH) grafted COF membrane (thickness ~800 nm) was fabricated on porous alumina through the vacuum filtration method.[140] Each pore aperture (pore size – 2.9 nm) in COF-9 was decorated with twelve –COOH functional groups, which heavily enhanced the hydrophilicity of the COF membrane and induced anionic porous nanochannels. The improved hydrophilicity enhanced the flow rate of water through the pores up to ~2260 L m^{-2} h^{-1} MPa^{-1} at 1 bar pressure. Moreover, the ordered negative charged mesoporosity of the COF-9 membrane allowed the size and charge-selective molecular separation from water. The exfoliated COF-9 nanosheets were further fabricated on the porous track-etched polycarbonate membrane support (TEPC) with a pore size of 200 nm. Various cationic tetraalkylammonium salts were size-selectively sieved through the negatively-charged intrinsic pores in the COF-9/TEPC composite membrane. The smaller tetra alkyl ammonium species such as NH_4, Me_4N, Et_4N, Bu_4N, and Hex_4N (8.2 Å) were selectively passed through the mesopores in the COF membranes. On the other hand, the tetra alkyl ammonium species like Oct_4N (10.9 Å) and $dodecy_4N$ (15.1 Å) were rejected by the membranes due to their relatively larger size.

5.4 Removal of chlorinated molecules

The catalytic membrane reactor is an advanced method for the disinfection of many toxic micropollutants including

chlorinated benzenes in water. Recently, a Pd nanoparticle embedded COF membrane (COF-AO) was developed for the effective dechlorination of water in a membrane-based microreactor.[141] The COF-AO membrane was synthesized through the post-synthetic modification of an allyl-decorated hydrazine-connected β-ketoenamine 2D-COF (COF-AO) with thiol-functionalized polysiloxane. The thiol group in the linear polymer chemically bonded with the Pd nanoparticle incorporating COF through the photo-induced thiol–ene click reaction. The polysiloxane-connected COF@Pd membrane-based microreactor detoxified the chlorinated water through continuous-flow catalysis at room temperature. Importantly, *p*-chlorophenol was completely converted into phenol (99%) through embedded Pd nanoparticle-mediated heterogeneous catalysis at the membrane level. The water solutions containing *p*-chlorophenol were continuously passed through the catalytic membrane several times for complete conversion into phenol. Several functionalized chlorinated benzene molecules were dechlorinated through the COF-AO membrane with 93–99% efficiency.

5.5 Removal of protein contaminants

The nanofiltration membrane suffers from protein fouling issues which cause serious drawbacks in the membrane performance and its application. The intense deposition of proteins on the surface of membranes due to the weak interactions between the porous material and proteins results in the blockage of the pores and causes overall reduction of the flow rate of the contaminated aqueous solution. Consequently, more energy is required to maintain the sufficient flow rate of the solvent through the membrane. In this aspect, it is critical to filter the protein contaminants from water to minimize membrane fouling. In 2019, a carboxyl functionalized COF was reported for the removal of potent proteins such as serum albumin and γ-globulin from the aqueous solution.[142] A carboxyl 2D-COF was fabricated into a mixed matrix membrane with polyacrylonitrile as a porous support. The COF acts as a nanofiller (0–0.8%) in the mixed matrix membrane. The hydrophilic carboxyl-decorated intrinsic pore walls (pore size ~2.8 nm) of the COF supported the transport of water molecules through the membrane and blocked serum albumin and γ-globulin proteins with rejection efficiencies of 81.9% and 99.4%, respectively.

5.6 Removal of radioactive pollutants

Recently, a COF-based mixed matrix membrane was reported for the removal of UO^{2+} from water.[143] The mixed matrix membrane was composed of a sulfonyl group functionalized COF and sulfonated-polyethersulfone (SPES) polymer. The numerous hydrophilic sulfonyl groups present in the membrane improved the flow rate of water with low diffusion resistance. The obtained $[NH_4]^+[COF\text{-}SO_3^-]$/SPES membrane was used for the extraction of uranium from acidic uranium aqueous solutions (at pH = 1) with a maximum adsorption capacity of 99.4 mg g^{-1}. The sulfonyl groups in the membrane weakly interact with the UO^{2+} ions during the separation process. The rejection efficiencies of UO^{2+} were found to be 92%, 87%, 80%, 76%, 72%, 65%, and 62% for the initial pollutant concentration of 26 ppm, 67 ppm, 103 ppm, 119 ppm, 292 ppm, 510 ppm, and 567 ppm, respectively.

5.7 Desalination

The marine aqueous body is the largest source of water, containing several precious minerals and salts. However, the direct consumption and utilities of marine water are not possible due to the high concentration of these minerals and salts in water. The separation of minerals and salts, generally known as the desalination process, has two benefits: 1) the marine water can be used as freshwater for consumption and other household and agricultural utilities and 2) the recovery of precious elements from water. In this regard, the desalination of marine water gains scientific attention for the development of energy-free and large-scale separation technologies. In this aspect, membrane-based desalination provides the advantages of continuous operation feasibility and commercial level filtration of saline water. The desalination membrane should possess microporosity for the effective removal of salts and minerals through molecular sieving. Therefore, the COF is an excellent candidate for the desalination process due to the tunable porosity. The NaCl rejection features of β-ketoenamine COFs were computationally demonstrated with 95% theoretical rejection capability.[45] Consequently, several COFs are reported as mixed membrane matrixes or thin-film composites for the desalination of water. Notably, the interfacial polymerization of the secondary amine-linked SNW-1 COF and the polyamide layer on the polyethersulfone support forms a thin film composite membrane for desalination application.[144] The solid-state interfacial synthesis was facilitated through the deposition and consequent polymerization of trimesoyl chloride and piperazine on the surface polyethersulfone membrane. The resultant PA-SNW-1/PES membrane with a water flux rate from 100 L m^{-2} h^{-1} MPa^{-1} to 192.5 L m^{-2} h^{-1} MPa^{-1} rejected 80% Na_2SO_4 from saline water. Besides, the SNW-1 COF nanoparticle embedded interfacially polymerized thin-film composite was also reported as a forward osmosis desalination membrane.[145] The outer selective hollow fiber membrane with amine-rich SNW-1 performed well with a water flux rate of 31.5 L m^{-2} h^{-1} MPa^{-1}. Again, the incorporation of –COOH functional groups into the COF was demonstrated for the improved flux of water (64.2 L m^{-2} h^{-1} MPa^{-}) due to the surface hydrophilicity of the membrane.[146] Recently, bilayer solvent interfacial synthesis of a hydrazine-linked β-ketoenamine COF deposited on the surface of poly(ethylene imine) modified polysulfone was reported.[147] In the bi-phase system, the hydrazine and PTSA were dissolved in water, and 1,3,5-triformyl phloroglucinol was dissolved in *n*-hexane solvent. A chemically modified polysulfone membrane separated the interface of the bilayer solvent. The

COFs have grown on this membrane with a film thickness of ~500 nm through the first and secondary growth synthetic steps. The COF thin-film TpHz/PES (pore size ~0.8 nm) composite acted as a Na_2SO_4 rejecter from water with a maximum efficiency of 58.3% and with a flow rate of 41.7 L m^{-2} h^{-1} MPa^{-1}. Moreover, $MgSO_4$, $CaCl_2$, $MgCl_2$ and NaCl were size-selectively removed from the aqueous solution with rejection efficiencies of 45.3%, 25.1%, 21.0% and 6.7%, respectively.

6. COF foams for water remediation

The COFs are explored for their intrinsic micro and mesoporosity induced uptake of molecular pollutants from

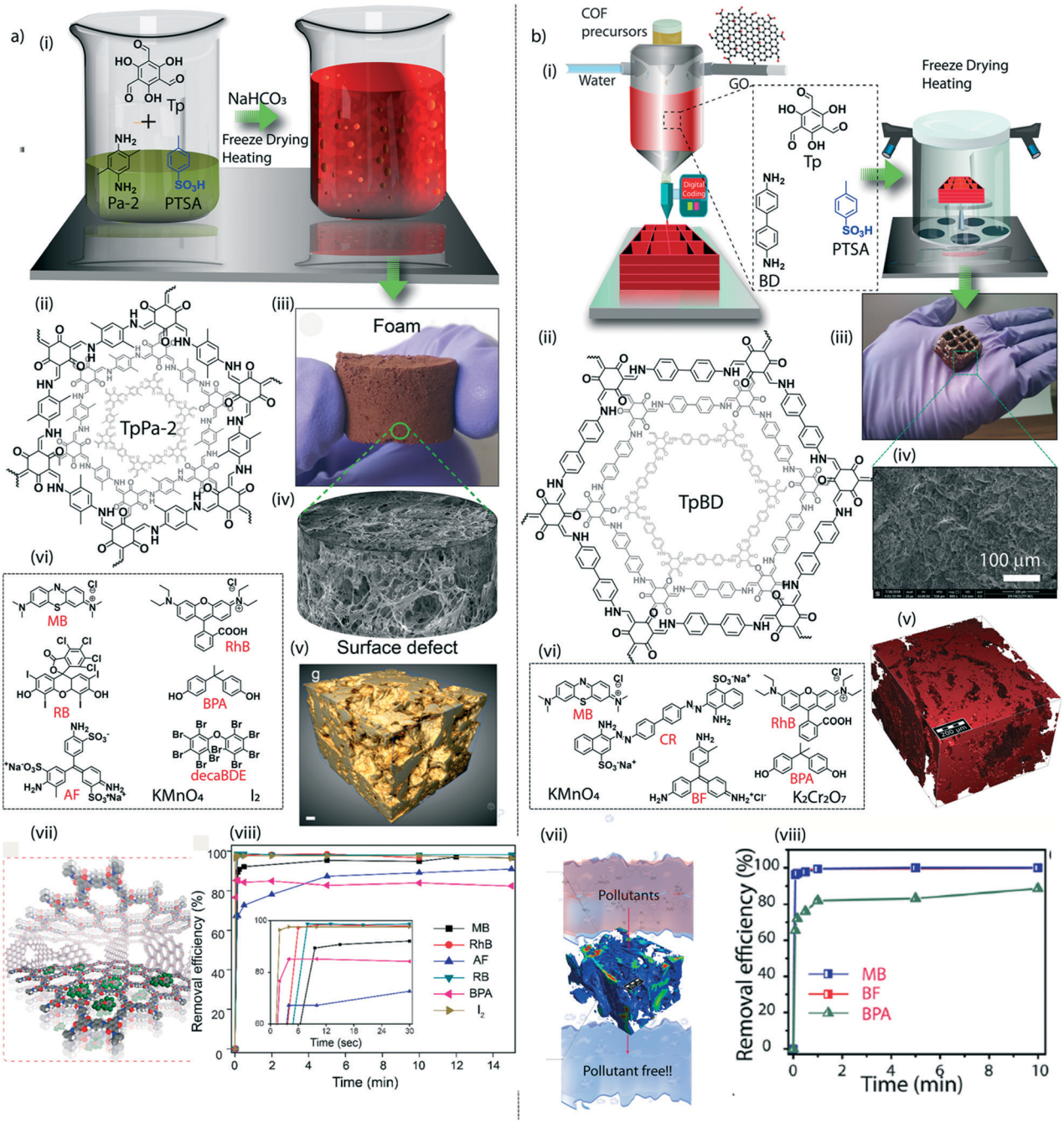

Fig. 8 a) (i) The diagrammatic representation of $NaHCO_3$ mediated COF foam synthesis, (ii) the Chem-Draw image of the TpPa-2 COF, (iii) the digital image, (iv) SEM and (v) 3D X-ray tomography image of COF foam, (vi) the pollutant molecules, (vii) the schematic diagram of pollutant uptake in foam, and (viii) the kinetic removal efficiency. b) (i) The diagrammatic representation of 3D-printed COF-GO foam synthesis, (ii) the Chem-Draw image of the TpBD COF, (iii) digital image, (iv) SEM and (v) 3D X-ray tomography image of COF foam, (vi) the pollutant molecules, (vii) the schematic diagram of pollutant uptake in foam, and (viii) the kinetic removal efficiency. [Reproduced from ref. 63 (Fig. 8aiii–v and vii and viii) and ref. 64 (Fig. 8biii–v and vii and viii) with permission from American Chemical Society, Copyright 2019 and Copyright 2020].

water. The ordered platform of these intrinsic pores facilitates the large surface area for the maximum adsorption of guest molecules through various interactions. In contrast, the ordered nature of the 2D-COF nanocrystallites hindered the rapid diffusion of molecules into the inner-core porous matrix of the material. The lower availability of macropores in crystalline 2D-COFs reduces the transportation feasibility of external molecules; hence it results in the incomplete utilization of the intrinsic framework pores. The physical states of COFs in membranes, 3D blocks, and even in granular forms face issues such as lack of connected macropores with the intrinsic meso and micropores. It could be due to the crystallite···crystallite interactions in the solid block of COFs without the presence of connected hierarchical porosity. The induction of macro, meso, and micropores in the COF matrix would enhance the rapid pore accessibility for guest molecules and has great potential in the removal of micropollutants from water.

Recently, the co-existence of micro, meso, and macropores in COFs was realized through the gas phase foaming of crystalline organic frameworks during the synthesis. The concurrent crystallization and engineering of the macropores in COFs was employed by adopting PTSA–$NaHCO_3$ mediated synthesis of four different β-ketoenamine COF foams (TpPa-2, TpPa-NO_2, TpAzo, and TpBD–Me_2-foams) (Fig. 8a).[63] The PTSA in the reaction mixture controlled the crystalline formation of the organic polymer. Meanwhile, the continuous effervescence of CO_2 molecules from $NaHCO_3$ was responsible for the hierarchical porosity of the resultant material. The 3D porous architecture of COF foam was strengthened by the removal of solvent water molecules through the freeze-drying cycles. The three-dimensionally scattered bubbling of CO_2 molecules in the reaction mixture placed the 2D layers far from each other. This disordered 3D-assembly of crystalline π–π stacked 2D layers offered the formation of several macropores with a range of porosity. The 3D distribution of macropores in the TpPa-2 COF foam was larger (67.7%) than the corresponding pristine COF (only 3.7%). Moreover, >99% of the macropores in the COF foam were interconnected in the entire porous matrix. In addition to the self-assembled mesopores (2.5–50 nm), the macroporous walls were built with microporous 2D-frameworks with a pore size less <2 nm. Additionally, the available mesopores further connected the hierarchical distribution of porosity in foams. Notably, this hierarchically connected porosity facilitated the rapid and efficient adsorption of a wide range of organic and inorganic micropollutants from water. The TpPa-2 foam takes up organic dye molecules such as MB, AF, and RB with ~99% efficiency and RhB with ~96% efficiency. The persistent organic pollutants such as decabromodiphenyl ether (~70%), inorganic pollutants like I_2 (~99%) and $KMnO_4$ (~96%), and the plastic pollutant bisphenol A (~79%) were also efficiently removed by COF foams. The purposefully made defects in the COF foams largely improved the kinetic efficiency of the adsorbent. The micropollutant removal reached equilibrium (with 90% efficiency) within 10 seconds of the adsorption period. In this study, the COF foams exhibited larger kinetics compared to the corresponding pristine COF. For example, 99% of MB was recovered by TpPa-2 COF foam within only 10 seconds, whereas the pristine TpPa-2 COF could remove only 70% even after 2 hours of adsorption. The pseudo-second-order rate constant (K_{obs}) of bisphenol A uptake by TpPa-2 foam (182.3 g mg^{-1} min^{-1}) was possibly due to the following reasons: 1) the smaller intrinsic pore size of the TpPa-2 COF, which efficiently accommodates similar size guest molecules and 2) the interconnected porosity expedites the transportation of guest molecules into the intrinsic micropores. Furthermore, the TpPa-2 COF foam was recycled for five cycles of consecutive MB uptake from water with preserved removal efficiency. A similar salt mediated gas-phase foaming approach has been adopted to fabricate an imine-linked TbBd foam (from 1,3,5-triformylbenzene as a C_3 knot and benzidine as a C_2 linker) for the removal of triphenylmethane organic dyes such as malachite green and crystal violet with maximum adsorption capacities of 172.4 mg g^{-1} and 149.3 mg g^{-1}, respectively.[148]

The construction of the large space extended 3D hierarchical porous architecture of crystalline organic polymeric materials is challenging because controlling the 3D growth often compromises their porosity, crystalline nature, and mechanical stability. The macroscopic architecture development of functional porous materials into 3D structures with desired size and shape shall be highly beneficial for energy-free separation and adsorption-based water remediation. Computational additive manufacturing (3D-printing) allows the fabrication of functional materials into pre-designed objects with large scalability. However, the undesirable rheological features of the semi granular nature of COF foams limited their 3D-printing features. The 3D-printing ink must possess the suitable properties of continuous flow and proper surface deposition with shear-thinning features. These challenges were addressed in the 3D-printing of hierarchical porous COF–GO foams where graphene oxide acts as a chemical spacer as well as the viscosity modifier of the ink (Fig. 8b).[64] The synthetic strategy of COF–GO foams implies the following steps: 1) the salt mediated β-ketoenamine (benzidine, 2, 6-diaminoanthraquinone, and 4,4′-azodianiline as C_2 linkers) monomer units in water were doped with graphene oxide as a foaming agent to achieve the self-assembly of microstructures, 2) the hydrogel ink was 3D-printed into pre-designed structures with the desired number of layers, and 3) the macroscopic architecture of the 3D-printed objects was subjected to the freeze-drying process. The hierarchical porosity of light-weight 3D-printed COF foams was derived from the mesoscale assembly of the microstructures such as crystalline COFs and graphene oxide. In addition to the BET microporous surface area (971 m^2 g^{-1}) which originates from the ordered intrinsic nanochannels (2–2.2 nm) of the COF, the macroporous surface area (TpBD foam: 44 414 m^2 m^{-3}) also contributed to the overall porosity of COF–GO foams.

The entire TpBD foam consists of 55% of macroporous void volume in which 90% of the macropores have a pore diameter in the range of 30–180 μm. On the other hand, the pristine TpBD COF can only have 11% of the macroporous volume ranging from 2 to 37 μm. The presence of a wide range of porosity in TpBD foam increased the rapid molecular diffusion into the surface of the material. The guest molecules non-covalently interacted with the pore walls and the periphery of COF foam crystallites. Owing to their hierarchically porous features, TpBD foam rapidly removed the organic micropollutant molecules such as MB (98%), CR (97%), RhB (73%), basic fuchsin (99%), and bisphenol A (76%) within 30 seconds. The inorganic molecules $KMnO_4$ (98%) and $K_2Cr_2O_7$ (55%) were also removed within 30 seconds of the adsorption period. Moreover, the maximum adsorption capacities of these organic pollutants in water were experimentally analyzed for MB (194 mg g^{-1}), basic fuchsin (310 mg g^{-1}), bisphenol A (69.6 mg g^{-1}), and RhB (194 mg g^{-1}). The adsorption kinetic analysis signified the rapid uptake of molecules from water. Moreover, the efficient regeneration performance of the foam over five cycles indicated its long-term use.

The sponge-like 3D monoliths of COF foam were fabricated for the removal of oil and organic solvents from water.[76] The anthraquinone-linked β-ketoenamine COF foam was synthesized through the PTSA catalysed reaction in the presence of reduced graphene oxide. The COF/rGO aerogel features a low-weight density (7 mg cm^{-3}) and high elasticity of the 3D porous network during mechanical compression (the strain developed up to 50% without any breaking of the structure). The COF/rGO aerogel selectively separates silicon oil from the oil–water mixture. Similarly, it also captured the chloroform solvent from water. The 1 : 1 ratio of COF/rGO aerogel adsorbed the solvent molecules 98 to 240 times to their weight.

The palladium (Pd) nanoparticle incorporating chitosan polymer support β-ketoenamine COFs were demonstrated for the dechlorination of chlorobenzene.[149] The COF crystallite embedded chitosan aerogel exhibited hierarchical porosity features which promoted the chlorobenzene molecule transport through the entire porous matrix. As a result, the molecules efficiently interacted with loaded Pd nanoparticles. The toxic chlorobenzene molecules were converted into corresponding phenols through Pd nanoparticle-based heterogeneous catalysis under ambient conditions. Notably, a large library of substituted chlorobenzene (–OH, $–OCH_3$, $–NH_2$, –CHO, –CN, $–COC_2H_5$, $–CO_2H$, and $–COCH_3$) molecules were dechlorinated with 93–99% yield. The recyclability of Pd@COF@chitosan for *p*-chlorophenol conversion was found for five catalytic cycles with 96% overall yield.

Conclusion

2D/3D COFs have been successfully explored as adsorbents and separating membranes for nano-level water treatment for the last five years. One of the notable achievements in this field is the development of excellent chemical stable COFs in water medium. The weak interaction chemistry of COFs with the contaminant molecules in water made them excellent adsorption and separation platforms in the pollutant filtration process. The granular 2D/3D COFs can be called the first generation of COF-based adsorbents for the remediation of water. Granular COFs have been extensively explored for the effective removal of a wide range of micropollutants including persistent organic pollutants, toxic metals, radioactive wastes, and pharmaceutical molecules. The recent research suggests that both the porosity and chemical functionality of COFs are the critical parameters to determine the efficiency of molecular adsorption. The selective removal of pollutants largely depends on the regulation of the pore size and the functional control over the framework. However, the porosity contribution of granular COFs majorly originated from the intrinsic nanochannels. Meanwhile, the macrophysical architecture development of COFs into foams allowed the inclusion of extrinsic meso and macroporosity. The hierarchical porosity in COF foams enhanced the efficiency and kinetics of micropollutant adsorption from water, which may be called the second generation of COF adsorbents. Moreover, COF foams were demonstrated as 3D-macroarchitectures. The COFs were also fabricated as thin and thick membranes for separation application. Both mixed matrix and free-standing membranes of COFs were studied for the separation of pollutant molecules. The successful implementation of COF membranes in organic micropollutant purification and desalination applications signifies the potential relevance of the material in water treatment. It is worth mentioning that the number of reports of COFs and their hybrid versions for water treatment has drastically increased in the last few years due to the potential features of the material.[150–154]

The macroscopic architecture of COFs is a promising research area, especially in water remediation technology. However, we believe that this field is still at the early stage and has vast opportunity to go beyond that. The molecular-level engineered macrostructures of COFs can be excellent candidates in the commercial-level treatment of water. Meanwhile, the advanced water purification technology demands selective, efficient, and rapid removal of a large library of emerging micropollutants with minimum energy consumption. In this regard, the researchers must tackle several tasks in this area to explore the full utilization of COFs in water operations. One of the main challenges that need to be addressed is the mechanical strength enhancement of higher-order macroscopic COFs. The nanocrystalline nature of COFs retards the mechanical stability and the flexibility of membranes and foams. The blending of additive foreign agents to improve the mechanical stability causes the mitigation in the surface area, hence resulting in poor performance in water treatment. Keeping this in perspective, it is important to improve the mechanical stability and flexibility of COF membranes and foams for commercial-level applications.

The fabrication of stretchable macrophysical forms of COFs is also recommended for further mechanical assistance.

Furthermore, creating smart-responsive macroscopic COFs will be a great opportunity to the window of light or electricity or mechanical simulated remediation of water. The smart responsive COF membranes or foams are expected to alter their porosity and functional features upon external stimuli; hence the control over pollutant removal can be finely regulated. The photo-, electro- or chemically induced degradation/conversion/adsorption of pollutants using COFs can be further explored in the smart-responsive macrostructure 2D/3D COFs. In addition, electrochemical desalination is an important area that demands extensive investigation to utilize the concurrent redox-active, electrical, and porous features of COFs in water treatment.[155] Although COFs are excellent materials for water purification, the cost of production is still not compromised compared to the existing adsorbents and membranes. We strongly suggest that the researchers give prime importance to the development of methods to reduce the cost of production of COF materials, especially in their macroscopic forms. The synthetic method should be economic and scalable. The novel functional and porous COFs, especially the advanced higher-order smart and robust macroscopic forms of COFs, can lead the future water treatment technology. We believe that the successful implementation of digitally controlled 3D-printing of this material into more complex and applicable shapes and sizes can tremendously change the story of water remediation.

Author contributions

A. K. M and D. S. conceptualized the review topic and the manuscript. A. K. M prepared the initial draft of the manuscript, and D. S. reviewed and edited it.

Conflicts of interest

There are no conflicts to declare.

Acknowledgements

This work was supported by Khalifa University Abu Dhabi. D. S. acknowledges financial support from a faculty startup grant (FSU-2020) and support under RCII-2018-024.

Notes and references

1 A. Boretti and L. Rosa, Reassessing the projections of the World Water Development Report, *npj Clean Water*, 2019, **2**, 15.
2 Y. Luo, W. Guo, H. H. Ngo, L. D. Nghiem, F. I. Hai, J. Zhang, S. Liang and X. C. Wang, A review on the occurrence of micropollutants in the aquatic environment and their fate and removal during wastewater treatment, *Sci. Total Environ.*, 2014, **473–474**, 619–641.
3 B. A. Wols and C. H. M. Hofman-Caris, Review of photochemical reaction constants of organic micropollutants required for UV advanced oxidation processes in water, *Water Res.*, 2012, **46**, 2815–2827.
4 C. Grandclément, I. Seyssiecq, A. Piram, P. Wong-Wah-Chung, G. Vanot, N. Tiliacos, N. Roche and P. Doumenq, From the conventional biological wastewater treatment to hybrid processes, the evaluation of organic micropollutant removal: A review, *Water Res.*, 2017, **11**, 297–317.
5 A. Alsbaiee, B. J. Smith, L. Xiao, Y. Ling, D. E. Helbling and W. R. Dichtel, Rapid removal of organic micropollutants from water by a porous beta-cyclodextrin polymer, *Nature*, 2016, **529**, 190–194.
6 Y. Tong, P. J. McNamara and B. K. Mayer, Adsorption of organic micropollutants onto biochar: a review of relevant kinetics, mechanisms and equilibrium, *Environ. Sci.: Water Res. Technol.*, 2019, **5**, 821–838.
7 J. Altmann, A. S. Ruhl, F. Zietzschmann and M. Jekel, Direct comparison of ozonation and adsorption onto powdered activated carbon for micropollutant removal in advanced wastewater treatment, *Water Res.*, 2014, **55**, 185–193.
8 W. Wan, R. Zhang, W. Li, H. Liu, Y. Lin, L. Li and Y. Zhou, Graphene–carbon nanotube aerogel as an ultra-light, compressible and recyclable highly efficient absorbent for oil and dyes, *Environ. Sci.: Nano*, 2016, **3**, 107–113.
9 Z. Tasic, G. Bogdanovic and M. Antonijevic, Application of natural zeolite in wastewater treatment: A review, *J. Min. Metall., Sect. A*, 2019, **55**, 67–79.
10 N. Koshy and D. N. Singh, Fly ash zeolites for water treatment applications, *J. Environ. Chem. Eng.*, 2016, **4**, 1460–1472.
11 J. H. Wendorff, The structure of amorphous polymers, *Polymer*, 1982, **23**, 543–557.
12 A. Schönhals and F. Kremer in *Polymer Science: A Comprehensive Reference*, ed. K. Matyjaszewski and M. Möller, Elsevier, Amsterdam, 2012, pp. 201–226.
13 B. Wang, Z. Xie, Y. Li, Z. Yang and L. Chen, Dual-functional conjugated nanoporous polymers for efficient organic pollutants treatment in water: asynergistic strategy of adsorption and photocatalysis, *Macromolecules*, 2018, **51**, 3443–3449.
14 H. Li, M. Eddaoudi, M. O'Keeffe and O. M. Yaghi, Design and synthesis of an exceptionally stable and highly porous metal-organic framework, *Nature*, 1999, **402**, 276–279.
15 B. Li, H. M. Wen, Y. Cui, W. Zhou, G. Qian and B. Chen, Emerging multifunctional metal-organic framework materials, *Adv. Mater.*, 2016, **28**, 8819–8860.
16 C. S. Diercks and O. M. Yaghi, The atom, the molecule, and the covalent organic framework, *Science*, 2017, **355**, eaal1585.
17 S. Kandambeth, K. Dey and R. Banerjee, Covalent organic frameworks: chemistry beyond the structure, *J. Am. Chem. Soc.*, 2019, **141**, 1807–1822.
18 X. Feng, X. Ding and D. Jiang, Covalent organic frameworks, *Chem. Soc. Rev.*, 2012, **41**, 6010–6022.

19 L. Joseph, B.-M. Jun, M. Jang, C. M. Park, J. C. Muñoz-Senmache, A. J. Hernández-Maldonado, A. Heyden, M. Yu and Y. Yoon, Removal of contaminants of emerging concern by metal-organic framework nanoadsorbents: A review, *Chem. Eng. J.*, 2019, **369**, 928–946.

20 A. Jeyaseelan and N. Viswanathan, Design of amino-functionalized benzene-1,4-dicarboxylic acid-Fabricated Lanthanum-Based Metal–Organic Frameworks fordefluoridation of water, *J. Chem. Eng. Data*, 2020, **65**, 5328–5340.

21 A. Jeyaseelan, Mu. Naushad, T. Ahamadbd and N. Viswanathan, Fabrication of amino functionalized benzene-1,4-dicarboxylic acid facilitated cerium based metalorganic frameworks for efficient removal of fluoride from water environment, *Environ. Sci.: Water Res. Technol.*, 2021, **7**, 384.

22 Z. Xia, Y. Zhao and S. B. Darling, Covalent organic frameworks for water Treatment, *Adv. Mater. Interfaces*, 2021, **8**, 2001507.

23 I. Ahmed and S. H. Jhung, Covalent organic framework-based materials: Synthesis, modification, and application in environmental remediation, *Coord. Chem. Rev.*, 2021, **441**, 213989.

24 A. P. Cote, A. I. Benin, N. W. Ockwig, M. O'Keeffe, A. J. Matzger and O. M. Yaghi, Porous, crystalline, covalent organic frameworks, *Science*, 2005, **310**, 1166.

25 S. J. Lyle, P. J. Waller and O. M. Yaghi, Covalent organic frameworks: organic chemistry extended into two and three dimensions, *Trends Chem.*, 2019, **1**, 172–184.

26 F. J. Uribe-Romo, J. R. Hunt, H. Furukawa, C. Klöck, M. O'Keeffe and O. M. Yaghi, A crystalline imine-linked 3-D porous covalent organic framework, *J. Am. Chem. Soc.*, 2009, **131**, 4570–4571.

27 Y. Liul, Y. Ma, Y. Zhao, X. Sun, F. Gándara, H. Furukawa, Z. Liu, H. Zhu, C. Zhu, K. Suenaga, P. Oleynikov, A. S. Alshammari, X. Zhang, O. Terasaki and O. M. Yaghi, Weaving of organic threads into a crystalline covalent organic framework, *Science*, 2016, **351**, 365–369.

28 Y. Jin, C. Yu, R. J. Denmana and W. Zhang, Recent advances in dynamic covalent chemistry, *Chem. Soc. Rev.*, 2013, **42**, 6634–6654.

29 S.-Y. Ding, J. Gao, Q. Wang, Y. Zhang, W.-G. Song, C.-Y. Su and W. Wang, Construction of covalent organic framework for catalysis: Pd/COF-LZU1 in Suzuki–Miyaura coupling reaction, *J. Am. Chem. Soc.*, 2011, **133**, 19816–19822.

30 S. Dalapati, S. Jin, J. Gao, Y. Xu, A. Nagai and D. Jiang, An azine-linked covalent organic framework, *J. Am. Chem. Soc.*, 2013, **135**, 17310–17313.

31 F. J. Uribe-Romo, C. J. Doonan, H. Furukawa, K. Oisaki and O. M. Yaghi, Crystalline covalent organic frameworks with hydrazone linkages, *J. Am. Chem. Soc.*, 2011, **133**, 11478–11481.

32 S. Kandambeth, A. Mallick, B. Lukose, M. V. Mane, T. Heine and R. Banerjee, Construction of crystalline 2D covalent organic frameworks with remarkable chemical (acid/base) stability via a combined reversible and irreversible route, *J. Am. Chem. Soc.*, 2012, **134**, 19524–19527.

33 P. Kuhn, M. Antonietti and A. Thomas, Porous, covalent triazine-based frameworks prepared by ionothermal synthesis, *Angew. Chem., Int. Ed.*, 2008, **47**, 3450.

34 X. Zhuang, W. Zhao, F. Zhang, Y. Cao, F. Liu, S. Bi and X. Feng, A two-dimensional conjugated polymer framework with fully sp2-bonded carbon skeleton, *Polym. Chem.*, 2016, **7**, 4176–4181.

35 E. Jin, M. Asada, Q. Xu, S. Dalapati, M. A. Addicoat, M. A. Brady, H. Xu, T. Nakamura, T. Heine, Q. Chen and D. Jiang, Two-Dimensional sp2 Carbon–Conjugated Covalent Organic Frameworks, *Science*, 2017, **357**, 673–676.

36 H. Lyu, C. S. Diercks, C. Zhu and O. M. Yaghi, Porous crystalline olefin-linked covalent organic frameworks, *J. Am. Chem. Soc.*, 2019, **141**, 6848–6852.

37 P. Hobza and J. Rezac, Introduction: Noncovalent Interactions, *Chem. Rev.*, 2016, **116**, 4911–4912.

38 J. L. Segura, S. Royuela and M. Mar Ramos, Post-synthetic modification of covalent organic frameworks, *Chem. Soc. Rev.*, 2019, **48**, 3903–3945.

39 M. Bhadra, S. Kandambeth, M. K. Sahoo, M. Addicoat, E. Balaraman and R. Banerjee, Triazine Functionalized Porous Covalent Organic Framework for Photo-organocatalytic E-Z Isomerization of Olefins, *J. Am. Chem. Soc.*, 2019, **141**, 6152–6156.

40 S. Y. Ding and W. Wang, Covalent organic frameworks (COFs): from design to applications, *Chem. Soc. Rev.*, 2013, **42**, 548–568.

41 Z. Li, X. Feng, Y. Zou, Y. Zhang, H. Xia, X. Liu and Y. Mu, A 2D azine-linked covalent organic framework for gas storage applications, *Chem. Commun.*, 2014, **50**, 13825.

42 C. R. DeBlase, K. E. Silberstein, T. T. Truong, H. D. Abruna and W. R. Dichtel, β-Ketoenamine-linked covalent organic frameworks capable of pseudocapacitive energy storage, *J. Am. Chem. Soc.*, 2013, **135**, 16821–16824.

43 M. A. Khayum, M. Ghosh, V. Vijayakumar, A. Halder, M. Nurhuda, S. Kumar, M. Addicoat, S. Kurungot and R. Banerjee, Zinc ion interactions in a two-dimensional covalent organic framework based aqueous zinc ion battery, *Chem. Sci.*, 2019, **10**, 8889–8894.

44 S. Kandambeth, B. P. Biswal, H. D. Chaudhari, K. C. Rout, H. S. Kunjattu, S. Mitra, S. Karak, A. Das, R. Mukherjee, U. K. Kharul and R. Banerjee, Selective molecular sieving in self-standing porous covalent-organic-framework membranes, *Adv. Mater.*, 2017, **29**, 1603945.

45 K. Zhang, Z. He, K. M. Gupta and J. Jiang, Computational design of 2D functional covalent–organic framework membranes for water desalination, *Environ. Sci.: Water Res. Technol.*, 2017, **3**, 735–743.

46 S. Yuan, X. Li, J. Zhu, G. Zhang, P. Van Puyvelde and B. Van der Bruggen, Covalent organic frameworks for membrane separation, *Chem. Soc. Rev.*, 2019, **48**, 2665–2681.

47 G. L. Dotto and G. McKay, Current scenario and challenges in adsorption for water treatment, *J. Environ. Chem. Eng.*, 2020, **8**, 103988.

48 M. S. Lohse and T. Bein, Covalent Organic Frameworks: Structures, Synthesis, and Applications, *Adv. Funct. Mater.*, 2018, **28**, 1705553.

49 L. M. Lanni, R. W. Tilford, M. Bharathy and J. J. Lavigne, Enhanced hydrolytic stability of self-assembling alkylated two-dimensional covalent organic frameworks, *J. Am. Chem. Soc.*, 2011, **133**, 13975–13983.

50 Y. Du, K. Mao, P. Kamakoti, P. Avikovitch, C. Paur, S. Cundy, Q. Li and D. Calabro, Experimental and computational studies of pyridine-assisted post-synthesis modified air stable covalent-organic frameworks, *Chem. Commun.*, 2012, **48**, 4606–4608.

51 S. Kandambeth, D. B. Shinde, M. K. Panda, B. Lukose, T. Heine and R. Banerjee, Enhancement of chemical stability and crystallinity in porphyrin-containing covalent organic frameworks by intramolecular hydrogen bond, *Angew. Chem., Int. Ed.*, 2013, **52**, 13052–13056.

52 H. Xu, J. Gao and D. Jiang, Stable, crystalline, porous, covalent organic frameworks as a platform for chiral organocatalysts, *Nat. Chem.*, 2015, **7**(11), 905–912.

53 P. F. Wei, M. Z. Qi, Z. P. Wang, S. Y. Ding, W. Yu, Q. Liu, L. K. Wang, H. Z. Wang, W. K. An and W. Wang, Benzoxazole-linked ultrastable covalent organic frameworks for photocatalysis, *J. Am. Chem. Soc.*, 2018, **140**, 4623–4631.

54 A. Halder, S. Karak, M. Addicoat, S. Bera, A. Chakraborty, S. H. Kunjattu, P. Pachfule, T. Heine and R. Banerjee, Ultrastable imine-based covalent organic frameworks for sulfuric acid recovery: an effect of interlayer hydrogen bonding, *Angew. Chem., Int. Ed.*, 2018, **57**, 5797–5802.

55 X. Guan, H. Li, Y. Ma, M. Xue, Q. Fang, Y. Yan, V. Valtchev and S. Qiu, Chemically stable polyarylether-based covalent organic frameworks, *Nat. Chem.*, 2019, **11**, 587–594.

56 C. Qian, W. Zhou, J. Qiao, D. Wang, X. Li, W. L. Teo, X. Shi, H. Wu, J. Di, H. Wang, G. Liu, L. Gu, J. Liu, L. Feng, Y. Liu, S. Y. Quek, K. P. Loh and Y. Zhao, Linkage engineering by harnessing supramolecular interactions to fabricate 2D hydrazone-linked covalent organic framework platforms toward advanced catalysis, *J. Am. Chem. Soc.*, 2020, **142**, 18138–18149.

57 A. Halder, M. Ghosh, M. A. Khayum, S. Bera, M. Addicoat, H. S. Sasmal, S. Karak, S. Kurungot and R. Banerjee, Interlayer hydrogen-bonded covalent organic frameworks as high-performance supercapacitors, *J. Am. Chem. Soc.*, 2018, **140**, 10941–10945.

58 H. Wang, C. Qian, J. Liu, Y. Zeng, D. Wang, W. Zhou, L. Gu, H. Wu, G. Liu and Y. Zhao, Integrating suitable linkage of covalent organic frameworks into covalently bridged inorganic/organic hybrids toward efficient photocatalysis, *J. Am. Chem. Soc.*, 2020, **142**, 4862–4871.

59 A. Nagai, Z. Guo, X. Feng, S. Jin, X. Chen, X. Ding and D. Jiang, Pore surface engineering in covalent organic frameworks, *Nat. Commun.*, 2011, **2**, 536.

60 A. R. Corcos, G. A. Levato, Z. Jiang, A. M. Evans, A. G. Livingston, B. J. Mariñas and W. R. Dichtel, Reducing the pore size of covalent organic frameworks in thin-film composite membranes enhances solute rejection, *ACS Mater. Lett.*, 2019, **1**, 440–446.

61 Y. Jin, Y. Hu and W. Zhang, Tessellated multiporous two-dimensional covalent organic frameworks, *Nat. Rev. Chem.*, 2017, **1**, 0056.

62 Z.-F. Pang, S.-Q. Xu, T.-Y. Zhou, R.-R. Liang, T.-G. Zhan and X. Zhao, Construction of covalent organic frameworks bearing three different kinds of pores through the heterostructural mixed linker strategy, *J. Am. Chem. Soc.*, 2016, **138**, 4710–4713.

63 S. Karak, K. Dey, A. Torris, A. Halder, S. Bera, F. Kanheerampockil and R. Banerjee, Inducing disorder in order: hierarchically porous covalent organic framework nanostructures for rapid removal of persistent organic pollutants, *J. Am. Chem. Soc.*, 2019, **141**, 7572–7581.

64 A. K. Mohammed, S. Usgaonkar, F. Kanheerampockil, S. Karak, A. Halder, M. Tharkar, M. Addicoat, T. G. Ajithkumar and R. Banerjee, Connecting microscopic structures, mesoscale assemblies, and macroscopic architectures in 3D-printed hierarchical porous covalent organic framework foams, *J. Am. Chem. Soc.*, 2020, **142**, 8252–8261.

65 J. Yin and B. Deng, Polymer-matrix nanocomposite membranes for water treatment, *J. Membr. Sci.*, 2015, **479**, 256–275.

66 J. W. Colson, A. R. Woll, A. Mukherjee, M. P. Levendorf, E. L. Spitler, V. B. Shields, M. G. Spencer, J. Park and W. R. Dichtel, Oriented 2D covalent organic framework thin films on single-layer graphene, *Science*, 2011, **332**, 228–231.

67 C. R. DeBlase, K. Hernández-Burgos, K. E. Silberstein, G. G. Rodríguez-Calero, R. P. Bisbey, H. D. Abruña and W. R. Dichtel, Rapid and efficient redox processes within 2D covalent organic framework thin films, *ACS Nano*, 2015, **9**, 3178–3183.

68 D. D. Medina, V. Werner, F. Auras, R. Tautz, M. Dogru, J. Schuster, S. Linke, M. Doblinger, J. Feldmann, P. Knochel and T. Bein, Oriented thin films of a benzodithiophene covalent organic framework, *ACS Nano*, 2014, **8**, 4042–4052.

69 M. A. Khayum, S. Kandambeth, S. Mitra, S. B. Nair, A. Das, S. S. Nagane, R. Mukherjee and R. Banerjee, Chemically delaminated free-standing ultrathin covalent organic nanosheets, *Angew. Chem., Int. Ed.*, 2016, **55**, 15604–15608.

70 H. Fan, J. Gu, H. Meng, A. Knebel and J. Caro, High-flux membranes based on the covalent organic framework COF-LZU1 for selective dye separation by nanofiltration, *Angew. Chem., Int. Ed.*, 2018, **57**, 4083–4087.

71 Z. Kang, Y. Peng, Y. Qian, D. Yuan, M. A. Addicoat, T. Heine, Z. Hu, L. Tee, Z. Guo and D. Zhao, Mixed matrix membranes (MMMs) comprising exfoliated 2D covalent organic frameworks (COFs) for efficient CO_2 separation, *Chem. Mater.*, 2016, **28**, 1277–1285.

72 K. Dey, M. Pal, K. C. Rout, H. S. Kunjattu, A. Das, R. Mukherjee, U. K. Kharul and R. Banerjee, Selective molecular separation by interfacially crystallized covalent organic framework thin films, *J. Am. Chem. Soc.*, 2017, **139**, 13083–13091.

73 M. Matsumoto, L. Valentino, G. M. Stiehl, H. B. Balch, A. R. Corcos, F. Wang, D. C. Ralph, B. J. Mariñas and W. R. Dichtel, Lewis-acid-catalyzed interfacial polymerization of covalent organic framework films, *Chem*, 2018, **4**, 308–317.

74 M. A. Khayum, V. Vijayakumar, S. Karak, S. Kandambeth, M. Bhadra, K. Suresh, N. Acharambath, S. Kurungot and R. Banerjee, Convergent covalent organic framework thin sheets as flexible supercapacitor electrodes, *ACS Appl. Mater. Interfaces*, 2018, **10**, 28139–28146.

75 Z. Wang, Q. Yu, Y. Huang, H. An, Y. Zhao, Y. Feng, X. Li, X. Shi, J. Liang, F. Pan, P. Cheng, Y. Chen, S. Ma and Z. Zhang, PolyCOFs: a new class of freestanding responsive covalentorganic framework membranes with high mechanical performance, *ACS Cent. Sci.*, 2019, **5**, 1352–1359.

76 C. Li, J. Yang, P. Pachfule, S. Li, M.-Y. Ye, J. Schmidt and A. Thomas, Ultralight covalent organic framework/graphene aerogels with hierarchical porosity, *Nat. Commun.*, 2020, **11**, 4712.

77 H. Li and J.-L. Brédas, Impact of structural defects on the elastic properties of two-dimensional covalent organic frameworks (2D COFs) under tensile stress, *Chem. Mater.*, 2021, **33**, 4529–4540.

78 S. Thomas, H. Li, C. Zhong, M. Matsumoto, W. R. Dichtel and J.-L. Bredas, Electronic structure of two-dimensional π-conjugated covalentorganic frameworks, *Chem. Mater.*, 2019, **31**, 3051–3065.

79 M. S. Lohse, T. Stassin, G. Naudin, S. Wuttke, R. Ameloot, D. De Vos, D. D. Medina and T. Bein, Sequential pore wall modification in a covalent organic framework for application in lactic acid adsorption, *Chem. Mater.*, 2016, **28**, 626–631.

80 F. Wania and D. Mackay, Peer reviewed: tracking the distribution of persistent organic pollutants, *Environ. Sci. Technol.*, 1996, **30**, 390A–396A.

81 W. A. Gebbink, L. van Asseldonk and S. P. J. van Leeuwen, Presence of emerging per- and polyfluoroalkyl substances (PFASs) in river and drinking water near a fluorochemical production plant in the Netherlands, *Environ. Sci. Technol.*, 2017, **51**, 11057–11065.

82 W. Ji, L. Xiao, Y. Ling, C. Ching, M. Matsumoto, R. P. Bisbey, D. E. Helbling and W. R. Dichtel, Removal of GenX and perfluorinated alkyl substances from water by amine-functionalized covalent organic frameworks, *J. Am. Chem. Soc.*, 2018, **140**, 12677–12681.

83 S. He, T. Zeng, S. Wang, H. Niu and Y. Cai, Facile synthesis of magnetic covalent organic framework with three-dimensional bouquet-like structure for enhanced extraction of organic targets, *ACS Appl. Mater. Interfaces*, 2017, **9**, 2959–2965.

84 K. Srogi, Monitoring of environmental exposure to polycyclic aromatic hydrocarbons: a review, *Environ. Chem. Lett.*, 2007, **5**, 169–195.

85 W. Ji, Y. S. Guo, H. M. Xie, X. Wang, X. Jiang and D. S. Guo, Rapid microwave synthesis of dioxin-linked covalent organic framework for efficient micro-extraction of perfluorinated alkyl substances from water, *J. Hazard. Mater.*, 2020, **397**, 122793.

86 A. Tkaczyk, K. Mitrowska and A. Posyniak, Synthetic organic dyes as contaminants of the aquatic environment and their implications for ecosystems: A review, *Sci. Total Environ.*, 2020, **717**, 137222.

87 N. Huang, P. Wang, M. A. Addicoat, T. Heine and D. Jiang, Ionic covalent organic frameworks: design of a charged interface aligned on 1D channel walls and its unusual electrostatic functions, *Angew. Chem., Int. Ed.*, 2017, **56**, 4982–4986.

88 Z. Li, H. Li, X. Guan, J. Tang, Y. Yusran, Z. Li, M. Xue, Q. Fang, Y. Yan, V. Valtchev and S. Qiu, Three-dimensional ionic covalent organic frameworks for rapid, reversible, and selective ion exchange, *J. Am. Chem. Soc.*, 2017, **139**, 17771–17774.

89 B. Garai, D. Shetty, T. Skorjanc, F. Gándara, N. Naleem, S. Varghese, S. K. Sharma, M. Baias, R. Jagannathan, M. A. Olson, S. Kirmizialtin and A. Trabolsi, Taming the topology of calix[4]arene-based 2D-covalent organic frameworks: interpenetrated vs noninterpenetrated frameworks and their selective removal of cationic dyes, *J. Am. Chem. Soc.*, 2021, **143**, 3407–3415.

90 X. Pan, X. Qin, Q. Zhang, Y. Ge, H. Ke and G. Cheng, N- and S-rich covalent organic framework for highly efficient removal of indigo carmine and reversible iodine capture, *Microporous Mesoporous Mater.*, 2020, **296**, 109990.

91 N. Mokhtari, M. Afshari and M. Dinari, Synthesis and characterization of a novel fluorene-based covalent triazine framework as a chemical adsorbent for highly efficient dye removal, *Polymer*, 2020, **195**, 122430.

92 T. Xu, S. An, C. Peng, J. Hu and H. Liu, Construction of large-pore crystalline covalent organic framework as high-performance adsorbent for rhodamine B dye removal, *Ind. Eng. Chem. Res.*, 2020, **59**, 8315–8322.

93 X. Zhu, S. An, Y. Liu, J. Hu, H. Liu, C. Tian, S. Dai, X. Yang, H. Wang, C. W. Abney and S. Dai, Efficient removal of organic dye pollutants using covalent organic frameworks, *AIChE J.*, 2017, **63**, 3470–3478.

94 G.-H. Ning, Z. Chen, Q. Gao, W. Tang, Z. Chen, C. Liu, B. Tian, X. Li and K. P. Loh, Salicylideneanilines-based covalent organic frameworks as chemoselective molecular sieves, *J. Am. Chem. Soc.*, 2017, **139**, 8897–8904.

95 R.-L. Wang, D.-P. Li, L.-J. Wang, X. Zhang, Z.-Y. Zhou, J.-L. Mu and Z.-M. Su, The preparation of new covalent organic framework embedded with silver nanoparticles and its applications in degradation of organic pollutants from waste water, *Dalton Trans.*, 2019, **48**, 1051.

96 F. Liu, C. Nie, Q. Dong, Z. Ma, W. Liu and M. Tong, AgI modified covalent organic frameworks for effective bacterial disinfection and organic pollutant degradation under visible light irradiation, *J. Hazard. Mater.*, 2020, **398**, 122865.

97 H. Xue, Z. Bi, J. Cheng, S. Xiong and Y. Wang, Coupling covalent organic frameworks and carbon nanotube membranes to design easily reusable photocatalysts for dye degradation, *Ind. Eng. Chem. Res.*, 2021, **60**, 8687–8695.

98 Y. Liu, Y. Ma, J. Yang, C. S. Diercks, N. Tamura, F. Jin and O. M. Yaghi, Molecular weaving of covalent organic frameworks for adaptive guest inclusion, *J. Am. Chem. Soc.*, 2018, **140**, 16015–16019.

99 J. L. Tang-Péronard, H. R. Andersen, T. K. Jensen and B. L. Heitmann, Endocrine-disrupting chemicals and obesity development in humans: A review, *Obes. Rev.*, 2011, **12**, 622–636.

100 Y. Li, C. X. Yang and X. P. Yan, Controllable preparation of core-shell magnetic covalent-organic framework nanospheres for efficient adsorption and removal of bisphenols in aqueous solution, *Chem. Commun.*, 2017, **53**, 2511–2514.

101 S.-W. Lv, J.-M. Liu, C.-Y. Li, N. Zhao, Z.-H. Wang and S. Wang, Two novel MOFs@COFs hybrid-based photocatalytic platforms coupling with sulfate radical-involved advanced oxidation processes for enhanced degradation of bisphenol A, *Chemosphere*, 2020, **243**, 125378.

102 V. Chander, B. Sharma, V. Negi, R. S. Aswal, P. Singh, R. Singh and R. Dobhal, Pharmaceutical compounds in drinking water, *J. Xenobiot.*, 2016, **6**, 5774–5774.

103 L. Huang, N. Mao, Q. Yan, D. Zhang and Q. Shuai, Magnetic covalent organic frameworks for the removal of diclofenac sodium from water, *ACS Appl. Nano Mater.*, 2020, **3**, 319–326.

104 Y. Du, X.-T. Lv, Q.-Y. Wu, D.-Y. Zhang, Y.-T. Zhou, L. Peng and H.-Y. Hu, Formation and control of disinfection byproducts and toxicity during reclaimed water chlorination: A review, *J. Environ. Sci.*, 2017, **58**, 51–63.

105 X.-M. Wang, W.-H. Ji, L.-Z. Chen, J.-M. Lin, X. Wang and R.-S. Zhao, Nitrogen-rich covalent organic frameworks as solid-phase extraction adsorbents for separation and enrichment of four disinfection by-products in drinking water, *J. Chromatogr. A*, 2020, **1619**, 460916.

106 T. Skorjanc, D. Shetty, F. Gándara, L. Ali, J. Raya, G. Das, M. A. Olson and A. Trabolsi, Remarkably efficient removal of toxic bromate from drinking water with a porphyrin–viologen covalent organic framework, *Chem. Sci.*, 2020, **11**, 845–850.

107 J. Guo, M. Venier, A. Salamova and R. A. Hites, Bioaccumulation of dechloranes, organophosphate esters, and other flame retardants in great lakes fish, *Sci. Total Environ.*, 2017, **583**, 1–9.

108 B. E. Bengtsson, M. Tarkpea, T. Sletten, G. E. Carlberg, A. Kringstad and L. Renberg, Bioaccumulation and effects of some technical triaryl phosphate products in fish and Nitocra Spinipes, *Environ. Toxicol. Chem.*, 1986, **5**, 853–861.

109 W. Wang, S. Deng, L. Ren, D. Li, W. Wang, M. Vakili, B. Wang, J. Huang, Y. Wang and G. Yu, Stable covalent organic frameworks as efficient adsorbents for high and selective removal of an aryl-organophosphorus flame retardant from water, *ACS Appl. Mater. Interfaces*, 2018, **10**, 30265–30272.

110 T. Yasumoto and M. Murata, Marine toxins, *Chem. Rev.*, 1993, **93**, 1897–1909.

111 V. Romero, S. P. S. Fernandes, L. Rodriguez-Lorenzo, Y. V. Kolen'ko, B. Espina and L. M. Salonen, Recyclable magnetic covalent organic framework for the extraction of marine biotoxins, *Nanoscale*, 2019, **11**, 6072–6079.

112 D. Kar, P. Sur, S. K. Mandai, T. Saha and R. K. Kole, Assessment of heavy metal pollution in surface water, *Int. J. Environ. Sci. Technol.*, 2008, **5**, 119–124.

113 A. Khan, S. Khan, M. A. Khan, Z. Qamar and M. Waqas, The uptake and bioaccumulation of heavy metals by food plants, their effects on plants nutrients, and associated health risk: a review, *Environ. Sci. Pollut. Res.*, 2015, **22**, 13772–13799.

114 J. Binkley and J. A. Simpson, 35 - Heavy metals in wastewater treatment processes, in *Handbook of Water and Wastewater Microbiology*, ed. D. Mara and N. Horan, Academic Press, London, 2003, pp. 597–610.

115 S. Y. Ding, M. Dong, Y. W. Wang, Y. T. Chen, H. Z. Wang, C. Y. Su and W. Wang, Thioether-based fluorescent covalent organic framework for selective detection and facile removal of mercury(II), *J. Am. Chem. Soc.*, 2016, **138**, 3031–3037.

116 Q. Sun, B. Aguila, J. Perman, L. D. Earl, C. W. Abney, Y. Cheng, H. Wei, N. Nguyen, L. Wojtas and S. Ma, Postsynthetically modified covalent organic frameworks for efficient and effective mercury removal, *J. Am. Chem. Soc.*, 2017, **139**, 2786–2793.

117 N. Huang, L. Zhai, H. Xu and D. Jiang, Stable covalent organic frameworks for exceptional mercury removal from aqueous solutions, *J. Am. Chem. Soc.*, 2017, **139**, 2428–2434.

118 L. Huang, R. Shen, R. Liu and Q. Shuai, Thiol-functionalized magnetic covalent organic frameworks by a cutting strategy for efficient removal of Hg (2+) from water, *J. Hazard. Mater.*, 2020, **392**, 122320.

119 Y. Li, C. Wang, S. Ma, H. Zhang, J. Ou, Y. Wei and M. Ye, Fabrication of hydrazone-linked covalent organic frameworks using alkyl amine as building block for high adsorption capacity of metal ions, *ACS Appl. Mater. Interfaces*, 2019, **11**, 11706–11714.

120 M. A. Rahman, H. Hasegawa and R. P. Lim, Bioaccumulation, biotransformation and trophic transfer of arsenic in the aquatic food chain, *Environ. Res.*, 2012, **116**, 118–135.

121 C.-H. Yang, J.-S. Chang and D.-J. Lee, Covalent organic framework EB-COF:Br as adsorbent for phosphorus(V) or arsenic(V) removal from nearly neutral waters, *Chemosphere*, 2020, **253**, 126736.

122 X. Zhong, Z. Lu, W. Liang and B. Hu, The magnetic covalent organic framework as a platform for high-performance extraction of Cr(VI) and bisphenol a from aqueous solution, *J. Hazard. Mater.*, 2020, **393**, 122353.

123 Y. Jiang, C. Liu and A. Huang, EDTA-functionalized covalent organic framework for the removal of heavy-metal ions, *ACS Appl. Mater. Interfaces*, 2019, **11**, 32186–32191.

124 N. Tang, J. Liang, C. Niu, H. Wang, Y. Luo, W. Xing, S. Ye, C. Liang, H. Guo, J. Guo, Y. Zhang and G. Zeng, Amidoxime-based materials for uranium recovery and removal, *J. Mater. Chem. A*, 2020, **8**, 7588–7625.

125 C. W. Abney, S. Liu and W. Lin, Tuning amidoximate to enhance uranyl binding: a density functional theory study, *J. Phys. Chem. A*, 2013, **117**, 11558–11565.

126 Q. Sun, B. Aguila, L. D. Earl, C. W. Abney, L. Wojtas, P. K. Thallapally and S. Ma, Covalent organic frameworks as a decorating platform for utilization and affinity enhancement of chelating cites for radionuclide sequestration, *Adv. Mater.*, 2018, **30**, 1705479.

127 W. R. Cui, C. R. Zhang, W. Jiang, F. F. Li, R. P. Liang, J. Liu and J. D. Qiu, Regenerable and stable sp(2) carbon-conjugated covalent organic frameworks for selective detection and extraction of uranium, *Nat. Commun.*, 2020, **11**, 436.

128 F. F. Li, W. R. Cui, W. Jiang, C. R. Zhang, R. P. Liang and J. D. Qiu, Stable sp(2) carbon-conjugated covalent organic framework for detection and efficient adsorption of uranium from radioactive wastewater, *J. Hazard. Mater.*, 2020, **392**, 122333.

129 W.-R. Cui, C.-R. Zhang, R.-H. Xu, X.-R. Chen, R.-H. Yan, W. Jiang, R.-P. Liang and J.-D. Qiu, High-efficiency photoenhanced extraction of uranium from natural seawater by olefin-linked covalent organic frameworks, *ACS ES&T Water*, 2021, **1**, 440–448.

130 C.-R. Zhang, W.-R. Cui, R.-H. Xu, X.-R. Chen, W. Jiang, Y.-D. Wu, R.-H. Yan, R.-P. Liang and J.-D. Qiu, Alkynyl-based sp2 carbon-conjugated covalent organic frameworks with enhanced uranium extraction from seawater by photoinduced multiple effects, *CCS Chem.*, 2021, **3**, 168–179.

131 W. R. Cui, C. R. Zhang, R. H. Xu, X. R. Chen, R. H. Yan, W. Jiang, R. P. Liang and J. D. Qiu, Low band gap benzoxazole-linked covalent organic frameworks for photo-enhanced targeted uranium recovery, *Small*, 2021, **17**, e2006882.

132 Q. Lu, Y. Ma, H. Li, X. Guan, Y. Yusran, M. Xue, Q. Fang, Y. Yan, S. Qiu and V. Valtchev, Postsynthetic functionalization of three-dimensional covalent organic frameworks for selective extraction of lanthanide ions, *Angew. Chem., Int. Ed.*, 2018, **57**, 6042–6048.

133 M. M. Pendergast and E. M. V. Hoek, A review of water treatment membrane nanotechnologies, *Energy Environ. Sci.*, 2011, **4**, 1946–1971.

134 L. Xu, J. Xu, B. Shan, X. Wang and C. Gao, TpPa-2-incorporated mixed matrix membranes for efficient water purification, *J. Membr. Sci.*, 2017, **526**, 355–366.

135 L. Valentino, M. Matsumoto, W. R. Dichtel and B. J. Marinas, Development and performance characterization of a polyimine covalent organic framework thin-film composite nanofiltration membrane, *Environ. Sci. Technol.*, 2017, **51**, 14352–14359.

136 W. Zhang, L. Zhang, H. Zhao, B. Li and H. Ma, A two-dimensional cationic covalent organic framework membrane for selective molecular sieving, *J. Mater. Chem. A*, 2018, **6**, 13331–13339.

137 Y. Li, Q. Wu, X. Guo, M. Zhang, B. Chen, G. Wei, X. Li, X. Li, S. Li and L. Ma, Laminated self-standing covalent organic framework membrane with uniformly distributed subnanopores for ionic and molecular sieving, *Nat. Commun.*, 2020, **11**, 599.

138 J. Yao, C. Liu, X. Liu, J. Guo, S. Zhang, J. Zheng and S. Li, Azobenzene-assisted exfoliation of 2D covalent organic frameworks into large-area, few-layer nanosheets for high flux and selective molecular separation membrane, *J. Membr. Sci.*, 2020, **601**, 117864.

139 H. Yang, L. Yang, H. Wang, Z. Xu, Y. Zhao, Y. Luo, N. Nasir, Y. Song, H. Wu, F. Pan and Z. Jiang, Covalent organic framework membranes through a mixed-dimensional assembly for molecular separations, *Nat. Commun.*, 2019, **10**, 2101.

140 V. A. Kuehl, J. Yin, P. H. H. Duong, B. Mastorovich, B. Newell, K. D. Li-Oakey, B. A. Parkinson and J. O. Hoberg, A highly ordered nanoporous, two-dimensional covalent organic framework with modifiable pores, and its application in water purification and ion sieving, *J. Am. Chem. Soc.*, 2018, **140**, 18200–18207.

141 B.-J. Yao, J.-T. Li, N. Huang, J.-L. Kan, L. Qiao, L.-G. Ding, F. Li and Y.-B. Dong, Pd NP-loaded and covalently cross-linked COF membrane microreactor for aqueous CBs dechlorination at room temperature, *ACS Appl. Mater. Interfaces*, 2018, **10**, 20448–20457.

142 P. H. H. Duong, V. A. Kuehl, B. Mastorovich, J. O. Hoberg, B. A. Parkinson and K. D. Li-Oakey, Carboxyl-functionalized covalent organic framework as a two-dimensional nanofiller for mixed-matrix ultrafiltration membranes, *J. Membr. Sci.*, 2019, **574**, 338–348.

143 G. Wu, Y. Liu, Q. Zheng, Z. Yu and F. Luo, Ultrahigh uranium extraction performance of COFs/SPES mixed matrix membranes at acidic medium, *J. Solid State Chem.*, 2020, **288**, 121364.

144 C. Wang, Z. Li, J. Chen, Z. Li, Y. Yin, L. Cao, Y. Zhong and H. Wu, Covalent organic framework modified polyamide nanofiltration membrane with enhanced performance for desalination, *J. Membr. Sci.*, 2017, **523**, 273–281.

145 S. Lim, N. Akther, V. H. Tran, T.-H. Bae, S. Phuntsho, A. Merenda, L. F. Dumée and H. K. Shon, Covalent organic framework incorporated outer-selective hollow fiber thin-film nanocomposite membranes for osmotically driven desalination, *Desalination*, 2020, **485**, 114461.

146 L. Xu, T. Yang, M. Li, J. Chang and J. Xu, Thin-film nanocomposite membrane doped with carboxylated covalent organic frameworks for efficient forward osmosis desalination, *J. Membr. Sci.*, 2020, **610**, 118111.

147 R. Wang, M. Wei and Y. Wang, Secondary growth of covalent organic frameworks (COFs) on porous substrates for fast desalination, *J. Membr. Sci.*, 2020, **604**, 118090.

148 J. Liu, G. Li, Y. Yu and X. Zhou, Hierarchically porous covalent organic framework for adsorption and removal of triphenylmethane dyes, *Microporous Mesoporous Mater.*, 2021, **312**, 110703.

149 F. Li, L.-G. Ding, B.-J. Yao, N. Huang, J.-T. Li, Q.-J. Fu and Y.-B. Dong, Pd loaded and covalent-organic framework involved chitosan aerogels and their application for continuous flow-through aqueous CB decontamination, *J. Mater. Chem. A*, 2018, **6**, 11140–11146.

150 D. Liu, K. Li, M. Li, Z. Wang, M. Shan and Y. Zhang, Moderately crystalline azine-linked covalent organic framework membrane for ultrafast molecular sieving, *ACS Appl. Mater. Interfaces*, 2021, **13**, 37775–37784.

151 Y. Zhang, J. Guo, G. Han, Y. Bail, Q. Ge, J. Ma, C. H. Lau and L. Shao, Molecularly soldered covalent organic frameworks for ultrafast precision sieving, *Sci. Adv.*, 2021, **7**, eabe8706.

152 J. Li, Y. Yang, W. Ma, G. Li, Q. Lu and Z. Lin, One-pot room-temperature synthesis of covalent organic framework-coated superhydrophobic sponges for highly efficient oil-water separation, *J. Hazard. Mater.*, 2021, **411**, 125190.

153 Y. Xiao, C. Ma, Z. Jin, J. Wang, L. He, X. Mu, L. Song and Y. Hu, Functional covalent organic framework for exceptional Fe^{2+}, Co^{2+} and Ni^{2+} removal: An upcycling strategy to achieve water decontamination and reutilization as smoke suppressant and flame retardant simultaneously, *Chem. Eng. J.*, 2021, **421**, 127837.

154 S. P. S. Fernandes, P. Kovář, M. Pšeničkа, A. M. S. Silva, L. M. Salonen and B. Espiña, Selection of covalent organic framework pore functionalities for differential adsorption of microcystin toxin analogues, *ACS Appl. Mater. Interfaces*, 2021, **13**, 15053–15063.

155 Y. Li, Z. Ding, X. Zhang, J. Li, X. Liu, T. Lu, Y. Yao and L. Pan, Novel hybrid capacitive deionization constructed by a redox-active covalent organic framework and its derived porous carbon for highly efficient desalination, *J. Mater. Chem. A*, 2019, **7**, 25305.